Journal of Marine Research, 68, 63–95, 2010

The relation between the duration and shape of internal wave groups

by S. A. Thorpe[1,2]

ABSTRACT

This paper discusses the effect of the shape of internal wave groups on their "duration" or "lifetime"—how long they retain their form before their component waves disperse. The methodology devised by Smith and Brulefert (2010) to study the dispersion of surface wave groups is extended to examine the dispersion of internal wave groups. To provide tangible examples, it is supposed that wave groups of ellipsoidal shape, symmetrical about a vertical plane, are generated in a uniformly stratified thermocline by moving periodic disturbances perturbing the base of an overlying mixed layer. The dispersion relation for internal waves is used to determine the group duration, taken as the time required for the volume of the group to approximately double through the fastest separation of its component waves. As well as allowing the orientation (inclination of their larger, major axis to the horizontal) and aspect ratio (that of the minor to major axis in a vertical plane) of wave groups to vary, their lifetimes are compared in two particular cases: Case A in which the length of the initial minor axes in the vertical plane of the groups is the same, and Case B in which groups are initially composed of the same number of waves. Two-dimensional groups and "three-dimensional groups" (the latter predominantly two-dimensional but of limited extent in one horizontal direction) are considered. As has been found for surface waves, the duration of internal wave groups does indeed depend upon their shape. In both Cases, groups with relatively small aspect ratio and, in Case B, groups with many waves usually have greater lifetimes than relatively large aspect ratio groups with few waves. Two-dimensional groups have greater lifetimes than three-dimensional groups. In many cases, the groups with the longest lifetime have their longer (major) axis inclined at an angle to the horizontal that is close to the inclination of the group velocity vector; in these cases the lines of constant phase of waves composing the groups are not (as is found for some surface wave groups) slanted with respect to the major axis of the groups, but parallel. Some long-lifetime groups are found to have their major axes inclined to the horizontal at an angle that is very close to that of the front of a packet of waves generated by the moving periodic disturbance at the foot of the mixed layer. In Appendix B it is shown that the ratio, n_p/n or n_m/n, of the number of waves that would be recorded as the group passes a fixed point or a vertical mooring, to the number of waves contained, instantaneously, within a wave group, depends on the shape of the group and on the ratio of the dominant wave phase speed to the group velocity of the group. A simple model described in Appendix C suggests how such slanted wave groups can be generated in the thermocline by moving, but transient, disturbances. The orientation of "scars," regions left by waves breaking in the wave groups, is

1. School of Ocean Sciences, Bangor University, Menai Bridge, Anglesey, LL59 5AB, United Kingdom.
2. Correspondence address: "Bodfryn," Glanrafon, Llangoed, Anglesey LL58 8PH, United Kingdom. ***email: oss413@sos.bangor.ac.uk***

examined in Appendix D. Except for near inertial waves with small aspect ratio, scars are generally close to being horizontal.

1. Introduction

Wave groups are composed of component waves spanning a limited, but finite, bandwidth in wavenumber. Traveling with different group velocities, these component waves generally result in an increase in the size of groups unless the process of dispersion is suppressed by nonlinear effects. Neglecting nonlinearity, the rate of increase in the dimensions of surface wave groups has recently been shown to depend on the shape of the groups, groups with a particular shape or orientation relative to the downwind direction in which the waves are propagating having the longest duration before their area is doubled and their shape changed substantially. Our objective is to discover whether groups of internal waves have similar properties.

Using a long-range phased-array Doppler sonar, Smith and Brulefert (2010) have observed surface wave groups in deep water that are slanted, so that the angle between the longer (or major) axis of the groups and the wind direction is about 60 deg. The crests of waves within groups travel down-wind but are orientated at an angle with respect to their group envelope, resulting in an echelon-shaped pattern of wave crests. The width of the slanted groups is very small, equal to about one wavelength. The groups consequently have an appearance rather like that of a set of waves in one half of a ship's wake. Such groups of waves are found to be of fairly common occurrence, appearing about 15–20 times per hour, in data collected at a fixed location between the Hawaiian islands of Kauai and Oahu.

Smith and Brulefert use the linear dispersion relation to examine the time taken for the waves in such groups of slanted waves to disperse. Since the methodology is to be followed later, a brief description is appropriate here. The analysis is, however, somewhat involved and, for ease of reference, further details are given in Appendix A. In accordance with observations, the waves are supposed to travel downwind with crest lines at right angles to the wind direction. The mean speed of wave groups is chosen to be a value that corresponds to that observed, 5 m s^{-1}, half the phase speed of the deep water waves and, during the period of their observations, also about half the wind speed. The value of the mean wavenumber of the waves is therefore fixed (by the dispersion relation). It is assumed that, initially at least, groups have an elliptical shape or plan-form and the ratio of the minor and major axes of the groups is set equal to the observed value (about 0.2). Smith and Brulefert allow the orientation of the minor axes with respect to the wind direction, ϕ_S say, to vary, seeking the angle at which the dispersion of the waves forming a group is least, or the duration of the group is greatest. The duration or lifetime of groups depends on the time taken for waves of wavenumbers slightly different from their mean to disperse, a time determined by the variation of group velocity with wavenumber as explained in Appendix A, and is defined as the time required for the area of the water surface covered by a wave group to approximately double. The duration is found to be greatest when the orientation of the group is close to that at which the variation of group velocity in the direction of the

minor X-axis is zero (i.e., $\Delta c_{gX} = 0$, where Δc_{gX} is defined in Appendix A), so there is no dispersion of waves in this direction. This occurs at $\phi_S \approx 27$ deg., so that the angle between the longer (or major) axis of the groups and the wind direction is about 60 deg., as observed. Although the greatest duration of groups increases as the relative length of their major axes increases, both the lifetime and the orientation of the groups, ϕ_S, predicted to have the longest duration compare very favorably with observations. The slanted wave groups are predicted, and observed, to have longer durations than have groups of waves with axes aligned across and down-wind (i.e., when $\phi_S = 0$), by a factor of about 2.8, even though the variation of the group velocity in the direction of the major Y-axis, Δc_{gY}, is zero when $\phi_S = 0$ (Appendix A).

These remarkable observations and supporting theory (even though linear!) suggest that types of waves other than surface waves may be formed, and might commonly be observed, because they have a structure that allows them to persist longest and travel farthest. Such groups are, in a sense, the most "stable." The purpose of this note is to explore the implications that this may have for internal waves. Internal waves traveling along a narrow thermocline in midwater have dispersion properties similar to those of surface waves and will therefore have similar group dispersion properties.[3] Unlike Smith and Brulefert's waves, however, waves traveling on a seasonal thermocline often have wavelengths much greater than the thermocline's depth and so more closely correspond to shallow-water, rather than the deep-water, surface waves examined by Smith and Brulefert. Such internal waves are *nondispersive,* at least in the limit in which their wavelength divided by the depth of the thermocline tends to infinity. Internal waves traveling through a uniformly stratified region have, however, very different dispersion properties from those of surface waves, and it is groups of such internal waves that are considered here.

Little is known of internal wave groups in the ocean, although they are evident, with associated density overturns, in data analyzed by Alford and Pinkel (2000) obtained using a CTD that is rapidly lowered from R/P *FLIP.* It is not yet possible to follow wave packets as they propagate through the ocean. Groups may be formed in at least three ways: by the occasional random superposition of waves propagating with similar wavenumbers and therefore frequencies within the body of the ocean; by the "Benjamin-Feir" type of instability of an existing internal wave train (Borisenko *et al.,* 1976; Thorpe, 1977); or by radiation from transient moving disturbances or regions of instability, within or at the boundaries of the ocean. (It is by the last of these mechanisms that groups are supposed to be generated in Section 2.) Groups composed of two wave trains that interact nonlinearly

3. The dispersion relation for interfacial waves is $\sigma^2 = gk(\rho_2 - \rho_1)t_1t_2/(\rho_2t_1 + \rho_1t_2)$, where σ is the frequency, k the wavenumber, ρ_1 and ρ_2 the densities in the upper and lower layers of depths h_1 and h_2, respectively, and $t_i = \tanh(kh_i)$ for i = 1, 2 (Hunt, 1961). In deep layers, kh_i tends to infinity and t_i to 1, for both i = 1 and 2, so $\sigma^2 = gk(\rho_2 - \rho_1)/(\rho_2 + \rho_2)$. This has the same form, $\sigma^2 = gk$, as the dispersion relation of surface gravity waves in deep water, but with a reduced acceleration due to gravity. If, however, kh_2 tends to infinity (deep lower layer) and kh_1 is small (wavelength $\gg h_1$), then σ^2 tends to $gk^2(\rho_2 - \rho_1)h_1/\rho_1$ and $c^2 = \sigma^2/k^2 = g(\rho_2 - \rho_1)h_1/\rho_1$; the phase speed, c, is related to water depth in the same way as is that for surface waves in shallow water. The group velocity, $\partial\sigma/\partial k$ is then independent of k and the waves are nondispersive.

may be relatively stable, or of "permanent form" (Thorpe, 2002a), but only if the interacting component wave trains lie in the same vertical plane. The effects of rotation contribute positively to such stability. Sutherland (2001, 2006) has examined the stability of packets of finite amplitude internal waves. He examines two-dimensional groups, those that vary in only one of the horizontal directions, and disregards the effects of the Earth's rotation. He examines groups that are horizontally periodic but of limited vertical extent and groups with axes of symmetry that are vertical and horizontal (a group orientation later denoted by $\phi = \pi/2$ or 0, neither of which are here found generally to be groups with the greatest possible duration). Among other results, Sutherland finds that groups are stable if their velocity of propagation (the wave group velocity) is inclined at an angle to the horizontal (later denoted by θ) that is less than 54.74 deg., and unstable otherwise. The spatial distribution of patches of water mixed by the breaking of internal waves traveling in groups is known to depend on the shape of the groups (Thorpe, 1999); wave groups can therefore affect the structure of mixing in the ocean and it is of some interest to know more of their possible properties.

Rather than examining the stability of waves or wave groups, which inevitably involves some nonlinear aspects of their behavior, we here address the simpler problem of how the time over which wave groups retain their form, i.e., their duration or lifetime, depends on their shape. The spreading of internal waves belonging to a group is assessed using the dispersion relation and following Smith and Brulefert's method of analysis. (The dispersion relation for internal waves propagating in a fluid of constant buoyancy frequency and zero shear is exact; no nonlinear terms are ignored as in the Smith and Brulefert's analysis.) For simplicity, the many possible interactions that may occur between waves within a group, with other external waves or with the steady or variable mean flows through which a group is passing, are disregarded.

Section 2 describes the dispersion of internal wave groups for which calculations are made in Section 3. Results are discussed in Section 4 where reference is made to the different, but related, problem of the dominant frequency of waves radiating from a turbulent layer. The difference between the number of waves, n, observed instantaneously in a group, and the number that would be recorded as the group propagates past a fixed point, n_p, or a vertical mooring, n_m, is discussed in Appendix B. The ratios, n_p/n and n_m/n, depend on c/c_g and on the shape of the group. A simple model of internal wave group generation is described in Appendix C. The orientation of "scars," regions that have been mixed and left by waves breaking in the wave groups, is examined in Appendix D.

2. Analysis

Although groups or "packets" of internal waves may be generated by any of the transient processes that produce internal waves (some of which are described by e.g., Thorpe, 1975), to provide a specific example we assume here that groups are generated as lee waves in the thermocline forced by moving, quasi-periodic, modulated, transient disturbances at the base of the overlying mixed layer. These disturbances might be a consequence of

Kelvin-Helmholtz billows (Pham *et al.,* 2009), of convection (Ansong and Sutherland, 2010), or of Langmuir circulation cells being advected across the wind direction by Ekman drift (Thorpe and Hall, 1982; Polton *et al.,* 2008). Both billows and Langmuir circulation cells are known to be variable and unsteady, occurring in packets with modulated structures. Billows are observed to amalgamate with neighbors in "knots" that occur typically at distances along the billows of about 4 times the billow wavelength (Thorpe, 2002b). The corresponding coherence scales of wind-aligned Langmuir circulation cells is undetermined although their pattern is known to be irregular (Thorpe, 1992), neighboring cells amalgamating in "Y junctions" (Farmer and Li, 1995), the variable structure being described by McWilliams *et al.* (1997) as "Langmuir turbulence."

The quasi periodic disturbances (Fig. 1a) are supposed to have a mean horizontal wave number k, in a horizontal direction, x, and move in this direction at a mean speed, U, above the stationary deep layer of constant buoyancy frequency, N, although, in view of the variability of billows or Langmuir cells, k and U are later allowed to have some variation about these means and disturbances to be of limited extent in the second horizontal direction, y. The magnitude of k and U, their modulations or change of amplitude in time, determine the shape of internal wave groups that are generated (Fig. 1b), in particular their orientation, defined below by the angle φ, and the ratio of their minor and major axes.

The z-axis is taken to be vertically upwards. Rotation is included and the Coriolis frequency is f. The properties of the internal waves are related to the periodic forcing disturbances. The lee waves have wavenumber (k, l, m) (the l component is included to allow for the modulations of the forcing disturbances in the y direction) and wave frequency, σ, where, from the exact dispersion relation,

$$\begin{aligned}\sigma &= [(N^2(k^2 + l^2) + f^2m^2)/(k^2 + l^2 + m^2)]^{1/2},\\ &= N\chi,\end{aligned} \tag{1}$$

where $\chi = kU/N$ (<1), since the horizontal phase speed of the waves, σ/k, matches that of the forcing, U. This dispersion relation is valid for waves of finite amplitude; e.g., Thorpe (1994), and, rearranging, leads to

$$m = [(k^2 + l^2)(1 - \chi^2)/(\chi^2 - F^2)]^{1/2}, \tag{2}$$

where $F = f/N$. Near-inertial waves with σ near f are generated when $\chi \approx F$, while the wave frequency is close to the buoyancy frequency, N, when $\chi \approx 1$. The group velocity is $\underline{c_g} = (c_{gx}, c_{gy}, c_{gz})$ where

$$c_{gx}(k, l, m) = \partial\sigma/\partial k = N(1 - F^2)km^2/K^3K_l = Nk(1 - \chi^2)/\chi K^2,$$

$$c_{gy}(k, l, m) = \partial\sigma/\partial l = N(1 - F^2)lm^2/K^3K_l = Nl(1 - \chi^2)/\chi K^2,$$

and

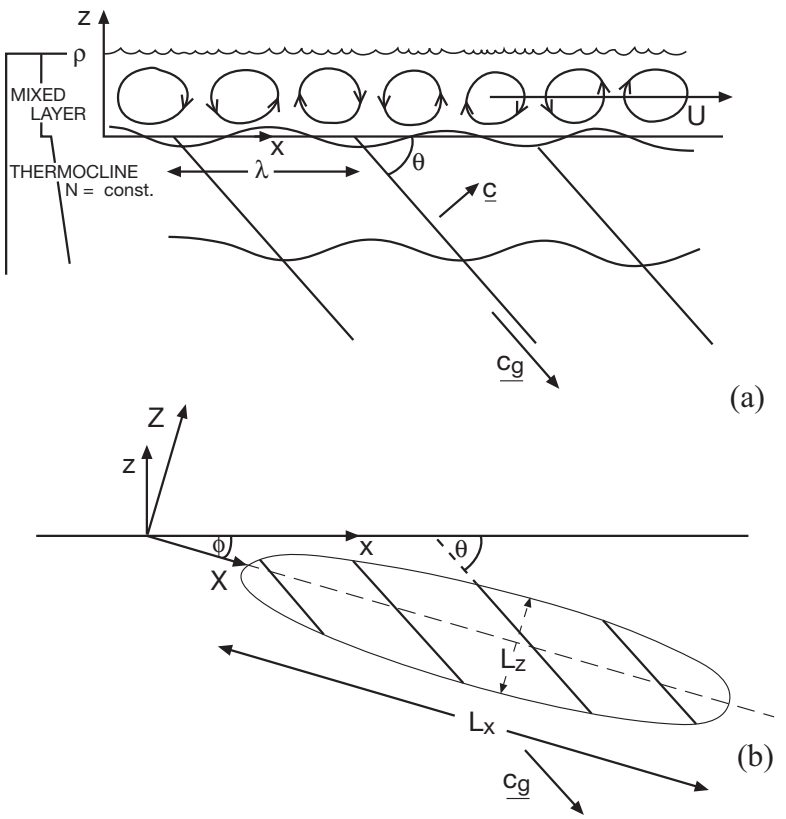

Figure 1. Internal waves, their surfaces of constant phase marked by tilted lines, generated by a localized, spatially periodic disturbance, such as the Langmuir cells sketched in (a), of wavelength, $\lambda = 2\pi/k$, moving (at right angles to their wind-aligned axes) in the x-direction at speed U in a mixed layer above a uniformly stratified region of buoyancy frequency, N. (a): lines of constant phase are inclined at angle, θ, to the horizontal. The phase velocity, $\underline{c}$, and the group velocity, $\underline{c_g}$ (parallel to lines of constant phase) are shown. (b): a group of waves with its major (X) axis inclined at angle ϕ to the horizontal. Its dimensions in the vertical X-Z plane are L_X and L_Z; $L_X > L_Z$. Modulations may also occur to the disturbance in the y-direction, and consequently the internal waves may be modulated (and the forced internal wave groups may be limited in their extent) in the Y-direction. The group advances in the direction $\underline{c_g}$.

$$\begin{aligned} c_{gz}(k, l, m) = \partial\sigma/\partial m &= -N(1 - F^2)m(k^2 + l^2)/K^3K_l \\ &= -N(\chi^2 - F^2)(1 - \chi^2)^{1/2}/[(1 - F^2)^{1/2}K\chi], \end{aligned} \tag{3}$$

with $K^2 = k^2 + l^2 + m^2$, $=(k^2 + l^2)(1 - F^2)/(\chi^2 - F^2)$ using (2), and $K_1 = [(k^2 + l^2) + m^2F^2]^{1/2}$. The group velocity is at right angles to the phase speed vector, $\underline{c} = (\sigma/K^2)(k, l, m)$, since $\underline{c}.\ \underline{c_g} = 0$.

The modulus of the group velocity is denoted as c_g:

$$c_g = N(1 - \chi^2)^{1/2}(\chi^2 - F^2)^{1/2}/K\chi. \quad (4)$$

If the horizontal wavenumber of the forcing disturbance in the y-direction is $l = 0$, wave groups travel at an angle $\tan^{-1}(-c_{gz}/c_{gx}) = k/m$ to the horizontal, given by

$$\theta = \tan^{-1}\{[(\chi^2 - F^2)/(1 - \chi^2)]^{1/2}\} \quad (5)$$

(see e.g., Thorpe, 2005), as sketched in Figure 1a. This direction depends on F and χ (or, for given N, on the product kU). The direction is normal to the phase velocity and therefore parallel to lines of constant phase. Modulations in the wavenumber and advection speed of the disturbance causing the generation of internal waves therefore lead to variations in the group velocity, c_g, and the propagation direction, θ, of the component waves of a wave group and, as we shall see later, to its spreading or dispersion.

The vectors $\underline{c}$ and $\underline{c_g}$ lie in the same vertical plane and if the x and z axes are chosen in this plane, it can be shown that

$$\underline{c} + \underline{c_g} = (N/\chi K)(\sin\theta, F^2\cos\theta), \quad (6)$$

the consequences of which will be apparent when wave breaking is discussed in Section 4.

Although the shape of a wave group will depend on how it is generated (an issue to which we return to in Section 4 and Appendix C), for generality we suppose an ellipsoidal shape, defining its orientation by choosing axes X and Z aligned along its longer (major) and shorter axes in the vertical plane containing the x and z axes, as in Figure 1b, with the major X axis inclined at an angle φ to the horizontal. The Y axis is in the y direction. The dimensions of the group in these directions are L_X, L_Y and L_Z, and the wavenumbers of the waves in the group are k_X, k_Y, and k_Z, respectively, where (by rotation of axes)

$$k = k_Z\sin\varphi + k_X\cos\varphi,\ m = k_Z\cos\varphi - k_X\sin\varphi \quad \text{and} \quad l = k_Y. \quad (7)$$

The three components of the group velocity in the X, Y and Z directions are

$$c_{gX} = c_{gx}\cos\varphi - c_{gz}\sin\varphi,\ c_{gY} = c_{gy} \quad \text{and} \quad c_{gZ} = c_{gx}\sin\varphi + c_{gz}\cos\varphi. \quad (8)$$

Two angles characterize wave groups generated by disturbances in the mixed layer. The angle θ defines the direction in which a group propagates, and there is a further angle, Φ, that defines the orientation of the front of a set of waves generated by a two-dimensional wave disturbance moving steadily in the x direction. As illustrated in Figure 2, waves generated at time $t = 0$ from a point A at $x = 0$ will have traveled to B, a distance $c_g t$ at an angle θ to the horizontal at a time, t, when waves are subsequently about to be generated at a point C where $x = Ut$. The line CB defines the front of the waves produced by a steadily moving disturbance of limited extent and is inclined at angle $-\Phi$ to the horizontal, where a negative sign is ascribed to Φ to make it consistent with the chosen sign of ϕ in Fig. 1b. Using the sine rule in triangle ABC we find

$$Ut/\{\sin[\pi - (\theta - \Phi)]\} = c_g t/\sin(-\Phi),$$

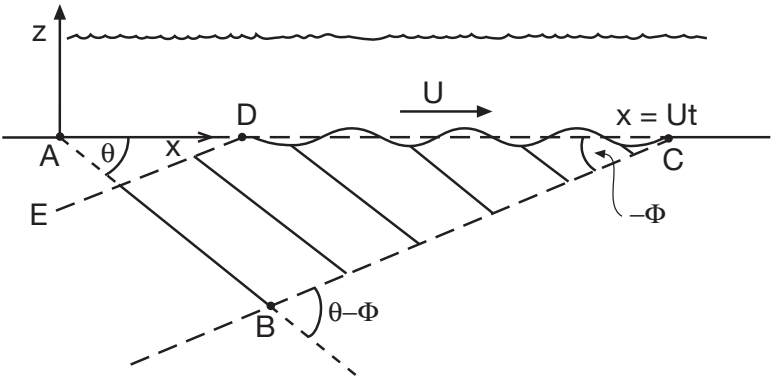

Figure 2. A packet of internal waves forced by a spatially periodic disturbance, CD, moving in the x-direction at speed, U. The line, CB, and the angle, Φ, defines the front of the advancing wave packet. The back of the packet is the line, DE. The point, A, marks the initial location of C.

which leads to

$$\tan\Phi = \sin\theta/(\cos\theta - U/c_g).$$

Substitution for θ and c_g using (4), (5) and (1) gives

$$\tan\Phi = -[(\chi^2 - F^2)^{3/2}(1 - \chi^2)^{1/2}]/(F^2 + \chi^4 - 2\chi^2F^2). \tag{9}$$

The angle θ defines the direction of propagation of wave groups radiating from a stationary periodic oscillation (Mowbray and Rarity, 1967) whilst Φ defines boundary lines of the front, CB (and back, DE), of a group generated by the movement of a disturbance, CD, moving steadily for a finite time. Figure 3 gives Φ and θ as functions of χ when $F = 10^{-2}$.

Appendix A describes how Smith and Brulefert calculate the duration of a surface wave group. Extending to internal waves in three-dimensions, we suppose that the wavenumber components k_X, k_Y, and k_Z are modulated as $k_X \pm \Delta k_X/2$, $\pm\Delta k_Y/2$ and $k_Z \pm \Delta k_Z/2$, where the amplitude of the wavenumber variations are related to the dimensions of the group:

$$\Delta k_X = 2\pi/L_X, \Delta k_Y = 2\pi/L_Y, \quad \text{and} \quad \Delta k_Z = 2\pi/L_Z. \tag{10}$$

By specifying the modulations in this way, groups have been selected that consist of waves that are of restricted extent in all three (x, y and z) directions but are periodic only in x and z. The groups considered here are specific to the periodic forcing by quasi two-dimensional disturbances and will differ from groups forced by, say, moving disturbances localized in x and y, (e.g., the pressure and stress caused by localized gusts of wind or those groups forced as lee waves around an isolated region of topography in a slowly varying flow). Groups with $\Delta k_Y = 0$, formed when the forcing has infinite extent in the y-direction i.e., $l = 0$, are referred to as "two-dimensional groups," otherwise they are "three dimensional." The wavenumber spectrum of waves in a wave group consists of a three-

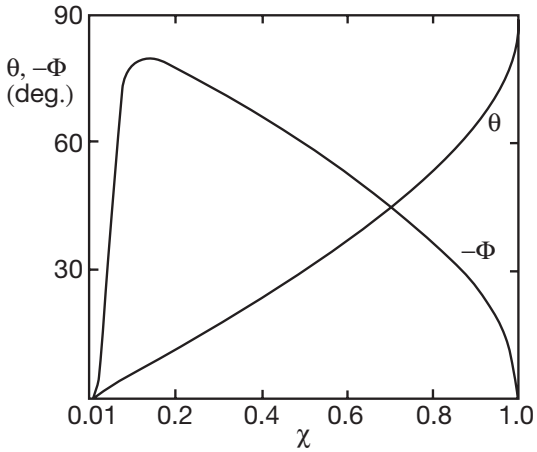

Figure 3. The angles θ and Φ (shown in Fig. 2) as a function of the forcing parameter, $\chi = kU/N$, when $F = 10^{-2}$.

dimensional region of high energy per unit wavenumber centered at k_X, k_Y (=0), and k_Z, and with dimensions $k_X \pm \Delta k_X/2$, $\pm\Delta k_Y/2$ and $k_Z \pm \Delta k_Z/2$ defining the range of wavenumbers of which the group is composed. The directional spectrum will generally be narrow, with a peak near the direction of the wavenumber $(k_X, 0, k_Z)$ or of the phase speed, $\underline{c}$, and at right angles to the direction, θ of the group velocity.

As shown by (3), unlike surface waves the group velocity of internal waves is not isotropic or, more significantly, monotonic in wavenumber, and the maximum speed of separation of a pair of waves belonging to a group (a speed that determines the group's lifetime) is not necessarily that of waves having the greatest separation in wavenumber. Instead of making a calculation as in (A1) of Appendix A, we calculate the difference between the group velocity components, Δc_{gX}, Δc_{gY} and Δc_{gZ}, over all pairs with wavenumbers, $(k_X + \delta\Delta k_X/2, \pm\Delta k_Y/2, k_Z + \varepsilon\Delta k_Z/2)$, belonging to a group, where $-1 \le \delta \le 1$ and $-1 \le \varepsilon \le 1$:

$$\Delta c_{gX} = c_{gX}(k_X + \delta_1\Delta k_X/2, \Delta k_Y/2, k_Z + \varepsilon_1\Delta k_Z/2) - c_{gX}(k_X + \delta_2\Delta k_X/2, -\Delta k_Y/2, k_Z + \varepsilon_2\Delta k_Z/2), \quad (11)$$

where δ_1 and ε_1, δ_2 and ε_2, all lie within -1 and 1 and define the wave pairs. The differences in Y and Z group velocities, Δc_{gY} and Δc_{gZ}, are defined similarly. Following Smith and Brulefert, the duration of a group, supposed ellipsoidal in shape, is defined as

$$T_d = (T_X^{-2} + T_Y^{-2} + T_Z^{-2})^{-1/2}, \quad (12)$$

where $T_X = L_X/|\Delta c_{gX}|$, $T_Y = L_Y/|\Delta c_{gY}|$ and $T_Z = L_Z/|\Delta c_{gZ}|$ represent the dispersal times in the three directions. This is a (biased and *ad hoc*) measure of the time required for the volume of a group to double which provides a useful measure for comparison. Because,

for example, the width of the group in a direction normal to the dominant wave crests within it may not double in this time—depending as T_d does on the difference in the group velocity components in the three directions, X, Y and Z—the number of waves within the group will not necessarily double in time, T_d. We seek the group velocity difference components that give the minimum T_d. Smaller group velocities lead to greater times before a group disintegrates through wave dispersion. The objective is to find the largest difference in group velocities, weighted as in (12), to determine the shortest time or group duration, before its component waves disperse or spread apart to a scale comparable to the initial dimensions of the group. In practice to make computational times sufficiently small, the differences in group velocity components are calculated as the values δ_i and ε_i, i = 1, 2, are varied between -1 and 1 in steps of 0.1.[4]

Since the wavenumber components in the (x, y, z) coordinates are related to those on the (X, Y, Z) coordinates (by (7)), variations Δk_X, Δk_Y and Δk_Z lead, via (1), to variations in $\chi = kU/N$ (and in σ), changes in the bandwidths and motion of the forcing disturbances must occur and correspond to the wavenumber variations within the groups. Physically, it is the variations in the forcing disturbances that lead to the structure of the internal wave groups. There is no component of group velocity normal to the lines of constant phase (or wave crests) of the dominant waves forming an internal wave group but, because there are variations in $\chi = kU/N$ (and in σ), there is a (relatively small) dispersion in this direction for the internal wave groups.[5] (We return to this point in Section 4.) It follows, however, that the length of wave crests may increase (relatively rapidly) and, consequently, the shape of wave groups may change in time.

Eqs. (11) (and similar equations for Δc_{gY} and Δc_{gZ}) and (12) can be expressed in terms of the X, Y and Z wavenumber components using (8), (3) and (7). Taking $\lambda = 2\pi/k$ (the wavelength of the forcing disturbance) and N^{-1} to nondimensionalize length and time scales, we can determine NT_d in terms of a set of parameters:

$\chi = kU/N$ (the parameter of the forcing, related by (1) to the frequency of the dominant waves in the group),

$q = L_Z/L_X$ (the aspect ratio of the group in the X-Z plane),

$\delta_Z = k/\Delta k_Z = L_Z/\lambda$ (the ratio of the dimension of the wave group in the Z direction to the disturbance wavelength, or a nondimensional measure of the width, L_Z, of the group),

$r^{-1} = L_Y/\lambda$ (the modulation scale in the y or Y direction divided by the disturbance wavelength; the inverse is taken so that $r = 0$ for "two-dimensional groups" with infinite extent in the *y* direction),

ϕ (the orientation of the wave group), and

4. It is found in many cases that δ_i and ε_i are equal to 1 or -1, implying that the wave pair leading to the greatest weighted differences in group velocity are indeed waves that are separated in wavenumber components as far as is possible within a wave group.

5. In the case of a surface wave group, there is no component of group velocity along the direction of the wave crests of the *dominant* waves, but (except when $\phi_S = 0$) some dispersion of the group in this direction owing to the finite bandwidth of the waves of which the group is composed.

$F = f/N$ (a measure of the effect of the Earth's rotation).

Values of these parameters must be chosen to conform with physical constraints. The value of χ must lie between F and 1 for m in (2) or θ in (5) to be real, so that freely radiating (rather than evanescent) lee waves are generated by the moving disturbance. The parameter r is later selected equal to 0 or to 0.25 to correspond most closely to the case when the forcing is by Kelvin-Holmholtz billows modulated in the y-direction at a scale of 4 times the billow wavelength.

The parameter δ_Z is related to the number of waves, n_X and n_Z, in the lengths, L_X and L_Z, in the X and Z directions of groups at any moment of time. Referring to the geometry of Figures 4a and b, the wavelengths, AB, are found from the sine rule applied to triangle ABC: $AB = \lambda\sin\theta/\cos(\theta - \varphi)$ in (a), which implies that the mean number of waves in L_Z is

$$n_Z = |\delta_Z\cos(\theta - \varphi)/\sin\theta|, \tag{13}$$

since $\delta_Z = L_Z/\lambda$. Similarly from (b), $AB = \lambda\sin\theta/\sin(\theta - \varphi)$ and n_X is given by

$$n_X = |\delta_Z\sin(\theta - \varphi)/q\sin\theta|, \tag{14}$$

using $q = L_Z/L_X$. For given forcing χ, these values depend on F only in so far as θ does through (6); they do not depend on the parameter, r, describing the effect of three-dimensionality. The number of waves in the X direction is zero when $\phi = \theta$, i.e., when the X-axis of the group is parallel to the lines of constant wave phase. (Examples of the variation of n_X and n_Z with ϕ for fixed δ_Z and q are given in Figure 6.)

The mean number of waves contained in a group, n, may be found if the shape of the group is supposed to be an ellipse with major and minor axes L_X and L_Z. It can be shown by simple geometry that the extent of the wave group in a direction normal to the wave crests, the distance D in Figure 4c, is equal to $[L_X^2\sin^2(\theta - \varphi) + L_Z^2\cos^2(\theta - \varphi)]^{1/2}$, and so the number of waves of wavelength $\lambda\sin\theta$ is $D/\lambda\sin\theta$, or

$$n = \delta_Z[\sin^2(\theta - \varphi) + q^2\cos^2(\theta - \varphi)]^{1/2}/(q\sin\theta), \tag{15}$$

using $\delta_Z = L_Z/\lambda$ and $q = L_Z/L_X$. Eq. (15) provides a relation between δ_Z and the number of waves in a group. The difference between the number of waves, n, observed instantaneously in a group, and the number that would be recorded as the group propagates past a fixed point, n_p, or a fixed vertical mooring line, n_m, is addressed in Appendix B. The ratios, n_p/n and n_m/n, depend on c/c_g and on the shape of the group.

If $T = 2\pi/\sigma$ is the wave period, the nondimensional duration, NT_d, is related through (1) to the duration divided by the wave period, or T_d/T (the number of wave periods for which a group retains its structure), by

$$T_d/T = NT_d(\chi/2\pi). \tag{16}$$

From (3), the vertical group velocity is when $l = 0$:

$$c_{gz} = -N(\chi^2 - F^2)^{3/2}(1 - \chi^2)^{1/2}/[k\chi(1 - F^2)]. \tag{17}$$

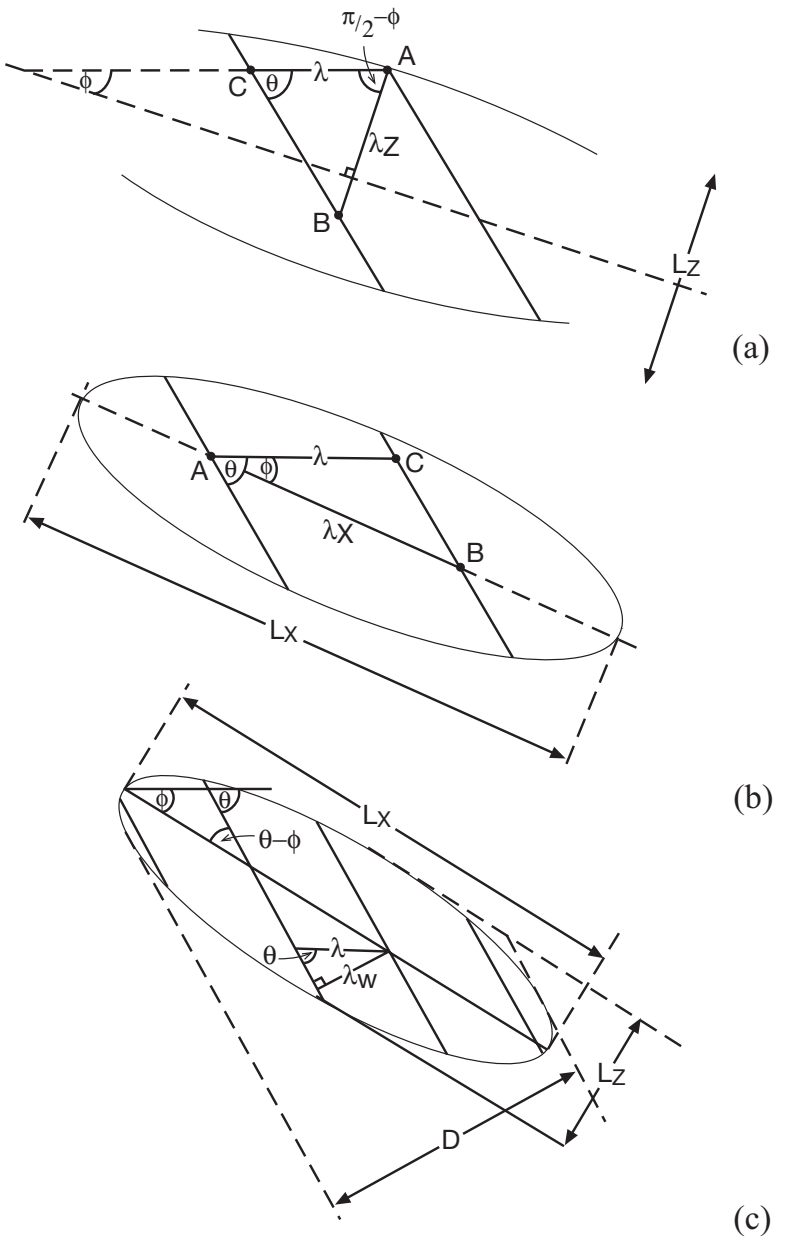

Figure 4. The number of waves in a group and their length. (a) and (b): the wavelength of waves in the Z and X directions, respectively. The wavelengths, λ_Z and λ_X, equal to AB, are found from the sine rule applied to triangle ABC. In (c) the group is represented as an ellipse with major and minor axes L_X and L_Z, the width of which, D, is equal to the distance between the two tangents at angle $(\theta - \phi)$ to the major axis. The mean number of waves in the group is D/λ_w, where $\lambda_w = \lambda\sin\theta$ is the wavelength.

For fixed k, the maximum of $-c_{gz}$ is found (by differentiation with respect to χ) at $\chi^2 = [1 + (1 + 3F^2)^{1/2}]/3$, so, for small F, $\chi \approx (2/3)^{1/2} \approx 0.816$ and from (5), $\theta \approx 54.74$ deg., the angle found by Sutherland to separate stable and unstable waves—see Section 1. (If, on the other hand, U is fixed, the maximum c_{gz} is found when $\chi \approx 2^{-1/2} \approx 0.707$, or $\theta \approx 45$ deg.)

The vertical distance, $z_{\max}$, through which a group travels downwards during its lifetime, T_d, is equal to $-c_{gz}T_d$. It may easily be shown using (17) that

$$z_{\max}/\lambda = (T_d/T)(\chi^2 - F^2)^{3/2}(1 - \chi^2)^{1/2}/[\chi^2(1 - F^2)]; \tag{18}$$

for given values of χ and F, the nondimensional measures, NT_d, $z_{\max}/\lambda$ and T_d/T, are therefore proportional to one another.

3. Results

Since there are 6 parameters, χ, q, δ_Z, r, ϕ and F, required to specify the shape and size of groups, some selection is needed in order to provide a simple comparison of the duration of groups of different shapes and orientations. The parameter F is chosen as 10^{-2}, typical of the upper ocean. The value of r is taken to be zero for two-dimensional groups or 0.25 for three-dimensional groups. The lifetimes of groups are now found and compared in two particular cases. In the first, Case A, the extent of a group in the Z direction, L_Z, is confined to a given fraction of the disturbance wavelength, λ: a set of values of δ_Z is chosen, each keeping the nondimensional group width, $L_Z/\lambda = \delta_Z$, constant. (The number of waves, n, in the groups will then vary.) In Case B, n is fixed to selected values and (15) is used to determine δ_Z.

Figure 5 shows how, in Case A, the logarithm of the nondimensional duration, NT_d, of groups with aspect ratio, $q = 0.2$, varies with their orientation, ϕ, and with the forcing disturbance, defined by χ and r, when nondimensional width is $\delta_Z = 1$. In Figure 5a, $r = 0$ so the forcing disturbance is uniform in the y-direction producing two-dimensional groups. Five different values of $\chi = kU/N$, are selected. There are generally two peaks in group duration, T_d. The durations vary by a factor of about 5 depending on the groups' orientation, ϕ. The durations, and in particular the maximum durations, decrease as the forcing frequency parameter, χ, increases (i.e., as the group propagation direction, θ, increases, as the wave frequency increases or the wave period decreases). The maximum duration occurs at a value of ϕ that varies with χ and is within 2 deg. of the group propagation direction, θ, given in Table 1, the exception being at $\chi = 0.8$ when the maximum duration is at a value of ϕ that is 5 deg. less than θ. The group duration for the values $q = 0.2$, $r = 0$ and $\delta_Z = 1$ shown in this figure does not show any particular behavior at an alignment corresponding to the front orientation, Φ (shown in Table 1). Here, and in later examples including those where the maximum duration is close to where $\phi = \Phi$, the maximum values of T_d occur close to values of ϕ where $|\Delta c_{gZ}|$ is small, i.e., where $T_Z = L_Z/|\Delta c_{gZ}|$ is very large. When $\phi = \theta$ and $l \approx 0$, it follows from (3) and (8)

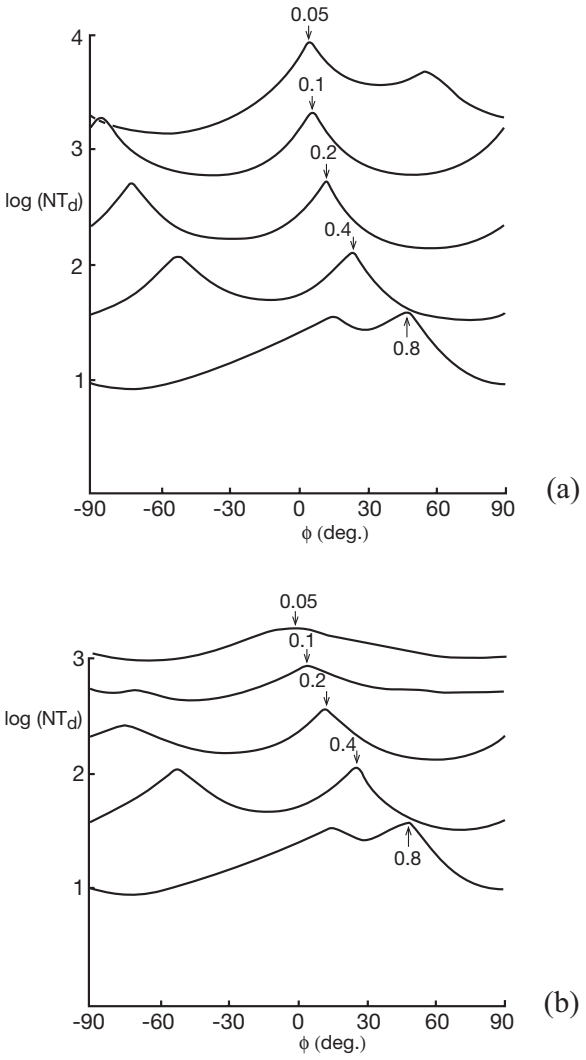

Figure 5. The nondimensional times, plotted in nondimensional form $\log(NT_d)$, as functions of group orientation, φ, for Case A when $q\ (=L_Z/L_X) = 0.2$, $F\ (=f/N) = 10^{-2}$, $\delta_Z = L_Z/\lambda = 1$, and at various labeled values of the forcing parameter, $\chi\ (=kU/N$; see Table 1), when (a) $r = 0$: the two-dimensional case when the group has infinite extent in the y- or Y-direction); and (b) $r = 0.25$. The maximum values of $\log(NT_d)$ are marked by arrows labeled with the corresponding values of χ.

that $c_{gZ} = 0$, and consequently Δc_{gZ} is small (but not necessarily zero, since the directional spectrum of the waves within the wave group, and therefore of the waves contributing to Δc_{gZ}, is of finite width; not all component waves have group velocity exactly in direction θ): a maximum of T_d for ϕ near θ therefore occurs close to where $|\Delta c_{gZ}|$ is small.

Table 1. The variation of the angles θ and Φ with χ when $F = 10^{-2}$

$\chi = kU/N$	θ (deg)	Φ (deg)
0.05	2.81	−48.00
0.10	5.71	−78.58
0.20	11.52	−77.78
0.40	23.57	−66.35
0.60	36.87	−53.13
0.80	53.13	−36.87

The value of the parameter, $r = \lambda/L_Y$, inversely proportional to the width of the group in the y or Y direction, is taken to be 0.25 in Figure 5b, corresponding most closely to the case when the forcing is by Kelvin-Holmholtz billows in or at the lower boundary of the mixed layer. As is seen by comparing Figures 5a and 5b, the effect of allowing dispersion in the y direction has little effect when $\chi > 0.2$, but reduces the variation in NT_d with ϕ, and reduces the maximum duration of the groups, when $\chi \leq 0.2$.

The total number of waves in the groups, n, given by (15), and the number of waves, n_X and n_Z, measured in the X and Z directions determined using (13) and (14), are shown in Figure 6 at three values of χ. Being independent of r, the numbers of waves are the same for parts (a) and (b) of Figure 5. The group size, measured by the number of waves it contains, varies with the orientation, ϕ, but, on average, decreases with the forcing parameter, χ. The groups containing the greater number of waves (those with the smaller χ) also have the largest maximum duration.

The general effects seen in Figure 5 are also apparent when the relative extent of the wave group, L_Z, is increased by a factor of 4, as shown in Figure 7 where $\delta_Z = 4$. Group durations are increased through the increase in δ_Z. The relative numbers of waves in the groups are proportional to δ_Z by (13)–(15), and are therefore 4 times greater than in Figure 6. The most obvious difference in trends is found by comparing Figures 5b ($r = 0.25$, $\delta_Z = 1$) and 7b ($r = 0.25$, $\delta_Z = 4$). The increase in δ_Z (or L_Z) greatly reduces the range of variation of NT_d as ϕ varies, and although the maximum values of NT_d decrease for $\chi \leq 0.4$, the maximum at $\chi = 0.8$ is greater than that at $\chi = 0.4$.

It is the maximum group durations or lifetimes of groups of set properties that are of greatest significance and importance in this study. Figure 8 shows, for Case A, the results of seeking the maximum duration of two-dimensional groups ($r = 0$) as the orientation, ϕ, is varied at set values of the group width, δ_Z, and forcing, χ. The orientation of the longest duration groups, ϕ_{max}, shown at the top of each part of the figure, has positive values that are very close to the propagation direction, θ, as noted earlier in relation to Figure 5a. There are also negative values of ϕ_{max} near Φ, corresponding to longest-lived groups that are tilted as are the wave fronts of Figure 2, possibly making them of a form more readily generated by moving disturbances, as described in Appendix C. The orientation also shows some tendency to increase (notably for values of q near 0.5 in Figure 8 parts b and c) as the aspect ratio, $q = L_Z/L_X$, of the groups increases (i.e., as the groups change from being

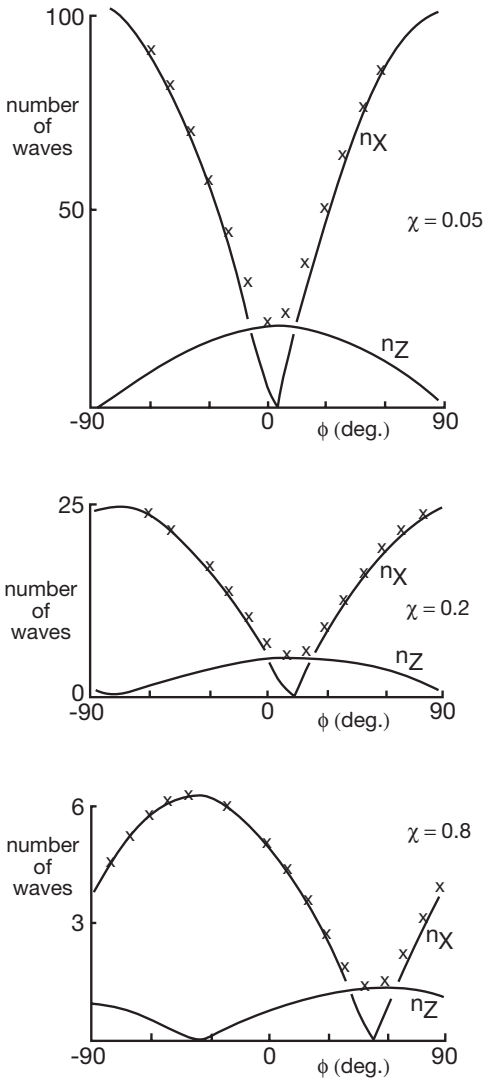

Figure 6. The number of waves in the groups, n (marked by crosses), and the number of waves, n_X and n_Z, in the X and Z directions in Case A plotted as functions of ϕ when (as labeled) $\chi = 0.05$, 0.2 and 0.8 and when $q\ (=L_Z/L_X) = 0.2$, $F\ (=f/N) = 10^{-2}$, $\delta_Z = L_Z/\lambda = 1$.

relatively long and thin to being more circular in form), but some abrupt changes with q of about $\pi/2$ occur in ϕ_{max}, e.g., near $q = 0.2$ and 1.0, resulting from jumps between the pairs of peaks of NT_d like those of Figures 5a and 7a. (As shown in Figure 3, the angles θ and Φ are separated by approximately $\pi/2$ when χ is greater than about 0.2.) The lower sections of each part of Figure 8 show duration measured by the logarithms of NT_d, the number of wave periods, T_d/T, and the maximum vertical distance over which they propagate, z_{max}/λ,

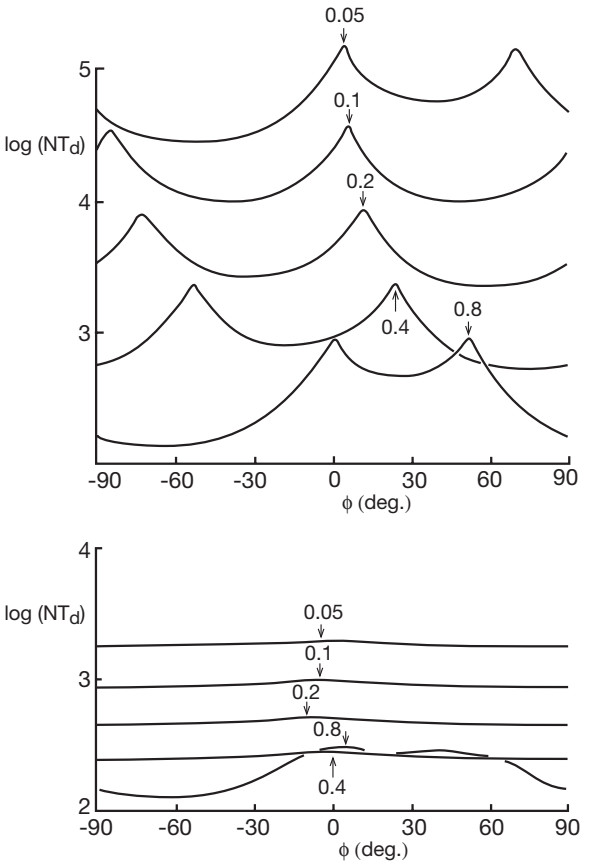

Figure 7. The nondimensional times, plotted in nondimensional form $\log(NT_d)$, as functions of group orientation, φ, for Case A as in Figure 5 but with $\delta_Z = L_Z/\lambda = 4$. (a) $r = 0$, and (b) $r = 0.25$. The number of waves, n, n_X and n_Z, in groups are 4 times those shown in Figure 6.

given by (18). All these nondimensional measures of duration decrease as q increases and as the group width, $L_Z/\lambda = \delta_Z$, decreases; the longest-lived groups have small aspect ratio, $q = L_Z/L_X$, and (perhaps not surprisingly) the wider the group, the longer is its duration. Similar results are found for three-dimensional groups with $r = 0.25$ as shown in Figure 9, although the nondimensional lifetimes of the groups, now shown on linear scales, are substantially smaller; it is again apparent that the effect of dispersion in the y direction is to reduce the lifetime of groups.

Effects of varying χ in three-dimensional groups when the width of groups is kept constant at $\delta_Z = 4$ are shown in Figure 10. Values of ϕ_{max} vary monotonically neither in q nor in χ, and (as already apparent in Figure 9) are not always near θ or Φ: the maximum propagation distance increases monotonically with χ when q is less than about 0.5, but has a maximum when $q > 0.6$ at a value of χ that decreases as q increases. This maximum is

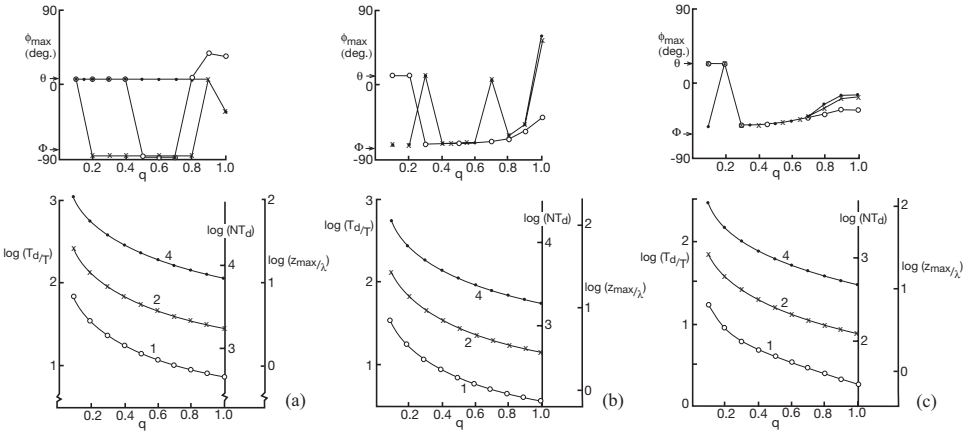

Figure 8. The variation of (top) the orientation of groups, $\phi = \phi_{max}$, when their duration, T_d, is greatest, and (bottom) the ratio of the maximum duration of the groups divided by the wave period, T_d/T, on a log scale, with the group shape parameter, $q = L_Z/L_X$, of two-dimensional ($r = 0$) groups in Case A at values of $\delta_Z = L_Z/\lambda = 4$ (dotted points), 2 (crosses) and 1 (circles), when $F = 10^{-2}$ and (a) $\chi = 0.1$, (b) $\chi = 0.2$, and (c) $\chi = 0.4$. Values of θ and Φ (given by Table 1) are marked by arrows on the ϕ_{max} axis. Scales for the values of $\log(NT_d)$ and $\log(z_{max}/\lambda)$ are also shown, inferred from T_d/T using (16) and (18).

perhaps not unexpected since (as mentioned in Section 2) internal waves have maximum vertical group velocity when $\chi = 0.707$ or 0.816, depending on whether U, or (as here) k, is kept constant. A dependence on the shape of groups (a variation with q) was not, however, foreseen.

In the second case, Case B, the number of waves in a group, n, is fixed. Values $n = 2$, 4, 8 or 16 are chosen and r is taken to be 0.25 in Figure 11, which shows the variation of

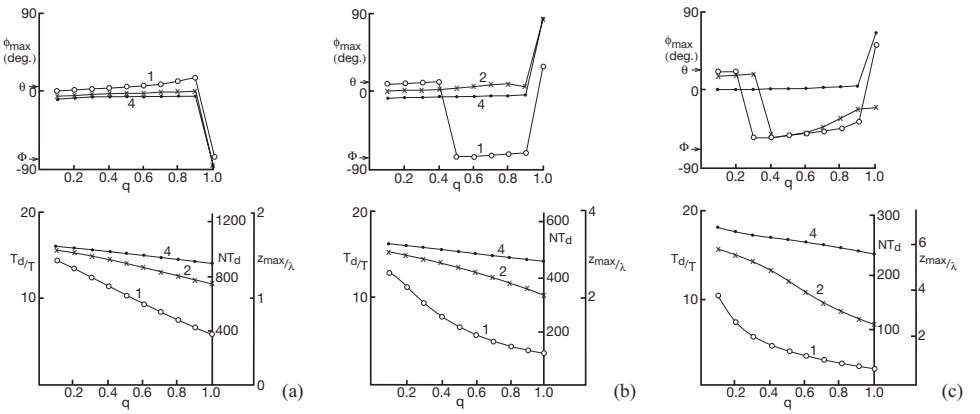

Figure 9. As in Figure 8, but for three-dimensional groups in Case A with $r = 0.25$, and with linear scales for T_d/T, NT_d and z_{max}/λ.

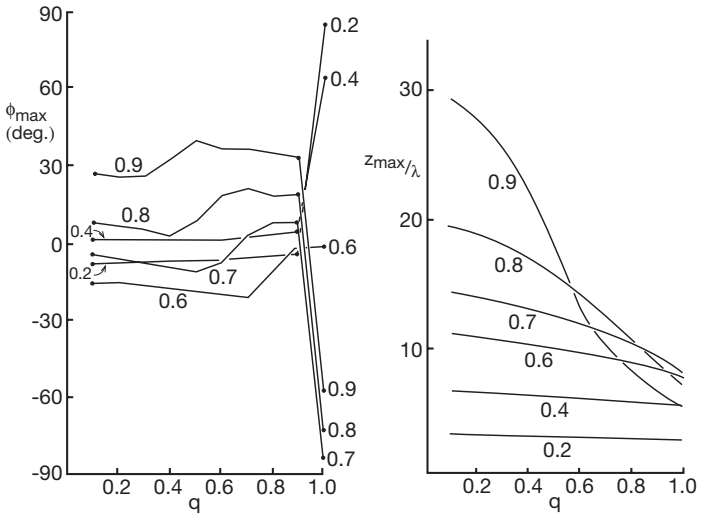

Figure 10. The variation of ϕ_{max} and z_{max}/λ (with a linear scale) with q for values of χ ranging from 0.2 to 0.9 (as labeled) when $\delta_Z = L_Z/\lambda = 4$ for three-dimensional groups with $r = 0.25$ in Case A as in Figure 9.

$\log(NT_d)$ with ϕ for a (labeled) set of values of χ when $q = 0.2$, the values selected earlier in Figures 5b and 7b. There are only two waves in a group (i.e., $n = 2$) in part (a). Values of T_d vary with ϕ by factors of about 100. The values, ϕ_{max}, where T_d reaches its maximum value increase with χ and, again, are near the group propagation direction, θ. Corresponding curves for $n = 8$ are shown in part (b). The maxima of T_d are greater than those when $n = 2$, but it is evident that the largest group durations do not vary monotonically with χ. Figure 12 shows values of ϕ_{max} and maximum durations for Case B for comparison with the earlier Figure 9 for Case A. Groups with few waves (i.e., $n = 2$) generally have longest durations when their orientation is near θ. The longest duration groups with many waves, $n = 16$, have $\phi_{max} < 0$ when $\chi = 0.2$ and 0.8, although no longer clustering near Φ. The durations NT_d and T_d/T, and the vertical propagation distance, z_{max}/λ, generally (but not always, e.g., for $n = 16$ in Figure 12b) decrease as q increases and as n decreases, and increase as χ increases.

4. Discussion

The main conclusion is that, as for surface waves, the duration of wave groups depends upon their shape. The longest lasting groups of equal relative widths, $\delta_Z = L_Z/\lambda$, are those with small values of aspect ratio, q, and (as shown in Figures 8, 9 and 12) are commonly inclined at an angle to the horizontal, $\phi = \phi_{max}$ (defined in Fig. 1b), that is very close to the propagation direction, θ (defined in Fig. 1a), or near the front angle, Φ (defined in Fig. 2). That the duration may be greatest near $\phi = \theta$ may be foreseen because $c_{gZ} = 0$ at this angle

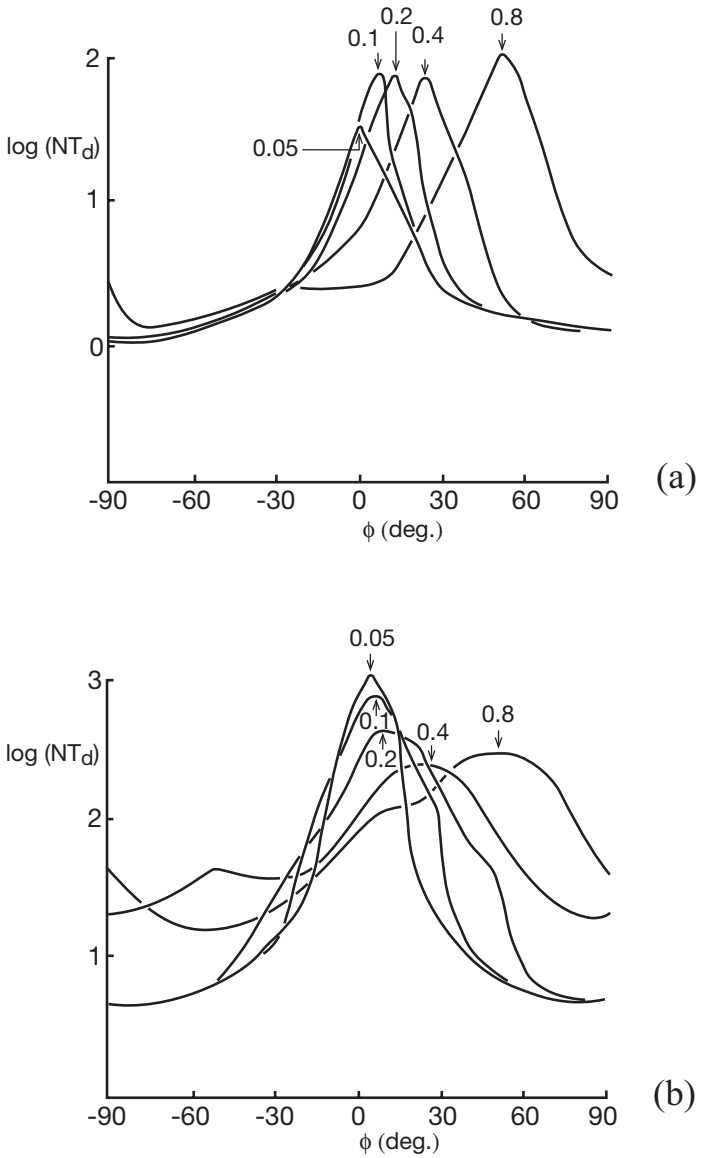

Figure 11. The nondimensional times, plotted in nondimensional form $\log(NT_d)$, as functions of group orientation, φ, when q $(=L_Z/L_X) = 0.2$, $F = 10^{-2}$, and at various values of the forcing parameter, χ, in case B when the number of waves in the three-dimensional ($r = 0.25$) group is (a) 2 and (b) 8. The maximum values of $\log(NT_d)$ are marked by arrows labeled with the corresponding values of χ.

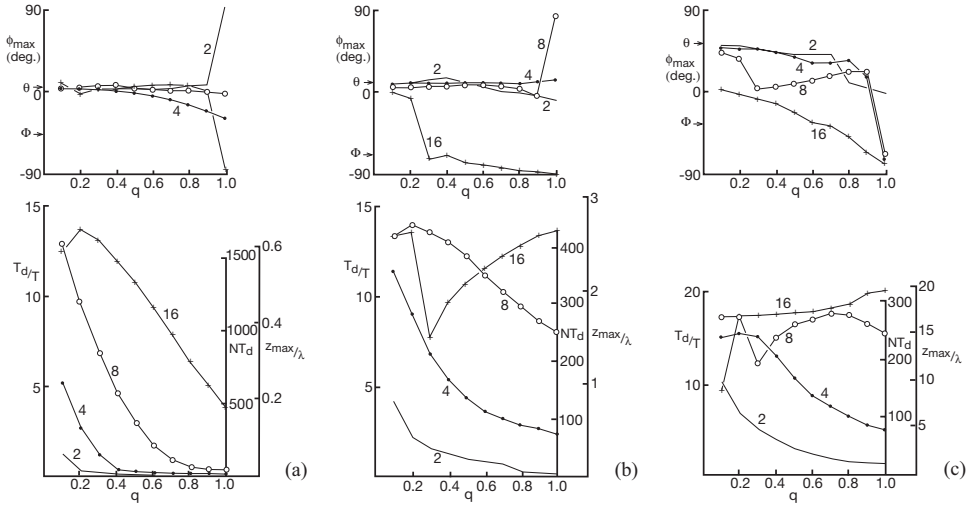

Figure 12. The variation with the group shape parameter, $q = L_Z/L_X$, of (top) the orientation of groups, $\phi = \phi_{max}$, when their duration, T_d, is greatest, and (bottom) the ratio of the maximum duration of the groups divided by the wave period, T_d/T, in Case B when the number of waves in the three-dimensional ($r = 0.25$) group is set at 2, 4, 8 and 16, as labeled. Values of the forcing parameter, χ, are (a) 0.05, (b) 0.2, and (c) 0.8. The curves $n = 4$ are marked by dots, $n = 8$ by circles and $n = 16$ by crosses. Values of θ and Φ (given by Table 1) are marked by arrows on the ϕ_{max} axis. As in Figure 8, values of NT_d and z_{max}/λ have been inferred from T_d/T using (16) and (18).

so Δc_{gZ} and T_Z^{-1} are relatively small, making T_d (12) relatively large. But, just as in the case of surface waves where there is no group velocity component along wave crests (suggesting—incorrectly—that $\phi_S = 0$ may give the maximum duration, even when, for surface waves, $\Delta k_Y = 0$; Appendix A), this is not necessarily the direction for *longest* duration.

Wide groups (measured by δ_Z; Case A) or groups with many waves (measured by n; Case B) generally have greater durations than relatively narrow groups with few waves. When $\phi \sim \theta$, the groups contain waves with lines of constant phase aligned along the major axes of the groups, and are like one of the (four) wave groups produced in the laboratory experiments by Mowbray and Rarity (1967) when their horizontal cylinder is oscillated in a uniformly stratified fluid a few times at a frequency less than N. In this case, and unlike Smith and Brulefert's surface wave groups, these waves are not slanted relative to the axes of the group.

Although the results in Cases A and B provide information about the inherent variation of the lifetime of internal wave groups with their shape, the assumption that δ_Z or n will be constant for groups of waves radiating from a moving turbulent mixed layer is untenable. A simple model is described in Appendix C that addresses the variations of δ_Z or n, as well as suggesting one way in which slanted groups with ϕ negative and near Φ might be formed.

The relation of groups and wave breaking was referred to in Section 1. Internal waves may break through many mechanisms (Staquet and Sommeria, 2002; Thorpe, 2005), for example by locally enhancing the shear and reducing the Richardson number below some critical value for a period long enough for billows to overturn (Troy and Koseff, 2005) or if they are steep enough to produce regions of static instability (Thorpe, 1994; Lombard and Riley, 1996). Suppose that waves traveling through a group break within some volume, V, that is advected within the group. The locus of the centre of the breaking region mapped out as the waves and group advance defines the region affected by wave breaking and mixing. A series of waves leaves behind a pattern of "scars" (i.e., regions mixed by the breakers). When V has a circular shape with an aspect ratio of unity, the scars are inclined to the horizontal at an angle $\phi_1 = \alpha$ where

$$\alpha = -\tan^{-1}(F^2\cot\theta), \tag{19}$$

in the direction of $\underline{c} + \underline{c_g}$ given by Eq. 6 (Thorpe, 1999). (The angle, α, is positive downwards when $\underline{c_g}$ is downwards as in Fig. 1.) For typical values of f/N, α is close to zero, so the scars are almost horizontal and the breaking waves result in horizontal mixed layers. An exception is when θ is small and $\sigma \approx f$ (i.e., for near-inertial waves) when $|\gamma|$ can be appreciable. The volume, V, is however likely to have a shape and axis-orientation similar to the wave group, and so in general, when $q \neq 1$, the aspect ratio of V will not be unity. The orientation of scars produced by two-dimensional wave groups is found in Appendix D. Scars produced by the longest duration, elliptically shaped groups are almost horizontal except for near-inertial waves when scars of groups with small aspect ratio, q, may be inclined at some 10 deg. (Fig. A4). Although small-scale active turbulence may be generated through the breaking of waves as a group travels through the fluid, it is unlikely to persist for the one wave period, $T = 2\pi/\sigma$, between the onset of breaking in successive waves of a group (Thorpe, 1999) except for waves of frequency near N; turbulence collapses after a time, τ, typically of order $10N^{-1}$ (Staquet and Godeferd, 1998), so that $\tau/T \approx 1.5\sigma/N$ which is <1 when σ/N is less than about 0.7. Turbulence generated at the beginning of wave breaking in one "scar" will rarely be sustained until the next wave starts to break. (Horizontal vortices created when turbulence imparts momentum to the fluid and small-scale density fluctuations may, however, persist for greater times; Thorpe, 2005.)

One important feature of the wave groups radiating downwards from the mixed layer is their transport of extreme values of wave slope or low Richardson number. Their duration and the vertical component of group velocity determine the depth to which such extremes are propagated or to which mixing produced directly by radiation of energy from the mixed layer in the form of wave groups can occur. As shown in Figures 9, 12 and A2, however, three-dimensional wave groups do not persist for very large times or propagate far except perhaps in the possibly rare cases in which groups contain many waves, n, have small aspect ratio, q, or have relatively large χ and consequently large propagation angles, θ, or when there is some nonlinear process that allows them to remain compact. The number of wave periods, T_d/T, for which three-dimensional groups even of the optimal shape persist

(and few groups may be generated with optimal form) are generally moderate. So too is the vertical propagation distance, z_{max}, before they cease to remain compact, measured in terms of the disturbance wavelength, λ. To provide a specific example: the mean (across-wind) distance between convergence regions of Langmuir cells in deep water is about 3 times the thickness of the mixed layer (Smith *et al.,* 1987). For a mixed layer 40-m thick, the corresponding disturbance wavelength, $\lambda = 2\pi/k$, is therefore about 120 m. If $N = 10^{-2}$ s^{-1}, a drift velocity, U, of about 3.8 cm s^{-1} transporting the Langmuir cells normal to the wind direction, gives $\chi = kU/N \approx 0.2$. Wave groups with the maximum duration for $\chi = 0.2$ are shown in Figure 9b, and have $11.0 < T_d/T < 16.3$ and $2.2 < z_{max}/\lambda < 3.4$ for δ_Z ranging from 1 to 4 and so, since $\lambda = 120$ m, $264 < z_{max}(\text{m}) < 408$. Corresponding values for Figure 12b are $2.5 < T_d/T < 13.9$ and $0.44 < z_{max}/\lambda < 2.8$ for n ranging from 2 to 16, giving $53 < z_{max}(\text{m}) < 334$. The maximum durations are not very large in terms of the period of the waves within the groups. Groups of waves generated in the manner selected here may therefore only rarely travel to substantial depths, and will propagate through the full water depth to reach and reflect from the seabed only where the water depth is much less than the mean depth of the ocean (about 3800 m).

A further factor prevents groups remaining coherent whilst propagating over large vertical distances. In the real ocean the buoyancy frequency varies in depth, and the dispersion relation of internal waves on which the analysis depends will (unlike that of surface waves in deep water) be dependent on location (Mathur and Peacock, 2009). Groups that have an "optimal" shape that leads to their having a maximum duration in the stratification of the upper themocline (or just above a benthic boundary layer mixed by Kelvin-Helmholtz billows, to which the analysis also applies), will change in shape through refraction as they propagate and become "nonoptimal." Nevertheless, the point made here is that the groups that persist longest (and may travel deepest) before dispersing may have a small aspect ratio, q, and inclination near θ or Φ, and that, like the slanted wave groups observed by Smith and Brulefert, the wave groups of greatest duration have a form that is unexpected.

It should be emphasized that the question addressed here concerns the duration of groups and the vertical distance over which wave groups retain their identity, rather than the depth to which internal waves of a given frequency transport energy from a turbulent region. Although both questions involve the vertical component of group velocity, the latter relates to the observation by Linden (1975) and Sutherland and Linden (1998) that waves generated in or at the boundaries of turbulent regions are found to radiate into their stratified, non-turbulent surroundings predominantly at angles, θ, of about 45 to 60 deg to the horizontal (see also Sutherland, 2001; Dohan and Sutherland, 2003, 2005; Taylor and Sarkar, 2007; Gayen *et al.,* 2010). That problem involves not only the rate of vertical transfer of energy, but the spectral distribution of wave energy generated by turbulence as well as the dissipation of wave energy, a feature not addressed in the present discussion. Waves will continue to propagate (retaining their frequency), to interact with other waves (possibly changing wave frequency), and to transfer energy even after the group structure

imposed during their generation at the base of the mixed layer has been lost through their relative dispersion. The present study is therefore linked, but not directly related or offering an answer, to the questions posed by Linden and Sutherland's observations.

It may be expected that the lifetime of groups of other types of waves, such as Rossby or Kelvin waves, also depend on their shape. The results draw attention to the need to discover more about internal wave groups: their shape, how persistent they are, and how they are produced.

Acknowledgments. This paper is based on Smith and Brulefert (2010), and I am grateful to Dr. Jerry Smith for letting me see a copy in advance of publication. I am also grateful to Professor Alan Davies for allowing me to use a computer and to Mrs. Kate Davis for assistance in producing the figures.

APPENDIX A

Smith and Brulefert's method of calculating the duration of surface wave groups

A wave group is, classically (e.g., Lighthill, 1978; Section 3.7), formulated as a sum of two waves of slightly differing wave numbers and frequencies so, for example, the wave amplitude is expressed as

$$\begin{aligned}\zeta &= a\exp\{\mathrm{i}[(k+\Delta k)\mathrm{x} + (\sigma-\Delta\sigma)\mathrm{t}]\} + a\exp\{\mathrm{i}[(k-\Delta k)\mathrm{x} + (\sigma-\Delta\sigma)\mathrm{t}]\},\\ &= 2a\exp[\mathrm{i}(k\mathrm{x}+\sigma\mathrm{t})]\cos(\Delta k\mathrm{x} + \Delta\sigma\mathrm{t}]\},\end{aligned}$$

representing a wave of the mean wavenumber and frequency, k and σ, modulated by the cosine term that has wavenumber and frequency, Δk and $\Delta\sigma$, and which advances in the x direction at speed $\Delta\sigma/\Delta k$, or, in the limit of small Δk and $\Delta\sigma$, at the group velocity. The modulation represents the wave group with a length $2\pi/\Delta k$. Extending to two-dimensions, Smith and Brulefert suppose that the wavenumber components k_X and k_Y are modulated as $k_\mathrm{X} \pm \Delta k_\mathrm{X}/2$ and $k_\mathrm{Y} \pm \Delta k_\mathrm{Y}/2$, where the amplitude of the wavenumber variations are related to the dimensions of the group, L_X and L_Y:

$$\Delta k_\mathrm{X} = 2\pi/L_\mathrm{X} \quad \text{and} \quad \Delta k_\mathrm{Y} = 2\pi/L_\mathrm{Y}.$$

The duration or lifetime of a group is determined by the time taken for a pair of waves belonging to the group to disperse. For the surface waves in deep water considered by Smith and Brulefert, the group velocity decreases monotonically with wavenumber and, since the dispersion relation is independent of direction, the group velocity is isotropic. The maximum rate of separation of two waves belonging to the group is therefore found from the difference in group velocities for the pair of waves that have the greatest and smallest wave numbers. For surface waves in an X-Y plane,

$$\Delta c_{g\mathrm{X}} = c_{g\mathrm{X}}(k_\mathrm{X} + \Delta k_\mathrm{X}/2, k_\mathrm{Y} + \Delta k_\mathrm{Y}/2) - c_{g\mathrm{X}}(k_\mathrm{X} - \Delta k_\mathrm{X}/2, k_\mathrm{Y} - \Delta k_\mathrm{Y}/2), \qquad \text{(A1)}$$

and $\Delta c_{g\mathrm{Y}}$ is defined similarly. For an elliptically shaped group Smith and Brulefert show that the duration of a group before waves disperse may be defined as

$$T_d = (T_\mathrm{X}^{-2} + T_\mathrm{Y}^{-2})^{-1/2},$$

where $T_X = L_X/|\Delta c_{gX}|$ and $T_Y = L_Y/|\Delta c_{gY}|$ represent the dispersal times in the two horizontal directions.

Observations show that the eccentricity of the wave groups is large so that $L_X \ll L_Y$ and Smith and Brulefert therefore put $\Delta k_Y = 0$. This implies that when the major axes of wave groups are aligned across-wind, parallel to the wave crests and in direction Y, $k_Y = 0$, there is no across-wind dispersion and $\Delta c_{gY} = 0$.

APPENDIX B

The number of waves observed in a group

The number of waves that are, instantaneously, in a group of dispersive waves, n, and the number recorded as the group passes a fixed point, n_p, generally differ.

A group of surface waves of length L_x in the (downwind) direction in which the waves travel, passes a fixed point in time L_x/c_g, where c_g is the group velocity. (The effects of dispersion and group elongation in the relatively short time taken for the group to pass the fixed point is neglected.) The number of waves of period, T, passing the point in this time is $n_p = L_x/Tc_g$. If the wavelength is λ, the average number of waves in the group is $n = L_x/\lambda$. Hence $n_p/n = \lambda/Tc_g = c/c_g$, since the phase speed, $c = \lambda/T$. For waves in deep water, $c_g = c/2$, and so $n_p/n = 2$; approximately twice as many waves are recorded at a fixed point as are actually present in a group.

A similar calculation can be made for an internal wave group, again ignoring dispersion. Suppose we take a point, A, through which the centre of an elliptical group illustrated as in Figure 4c propagates. The width of the group in the propagation direction, c_g, is found by simple geometry to be $W = L_X L_Z/[L_X^2\sin^2(\theta - \varphi) + L_Z^2\cos^2(\theta - \varphi)]^{1/2}$. The time taken to pass point A is therefore $L_X L_Z/[L_X^2\sin^2(\theta - \varphi) + L_Z^{2\cos^2}(\theta - \varphi)]^{1/2}/c_g$, where c_g is the group velocity of the group, e.g., as given by (4). If the wave period is T, the number of waves passing A in this time is

$$n_p = L_X L_Z/[L_X^2\sin^2(\theta - \varphi) + L_Z^2\cos^2(\theta - \varphi)]^{1/2}Tc_g.$$

But the number of waves in the wave group, n, is given by (15). This can be written as

$$n = [L_X^2\sin^2(\theta - \varphi) + L_Z^2\cos^2(\theta - \varphi)]^{1/2}K/2\pi,$$

where K is the wavenumber, and so

$$n_p/n = 2\pi L_X L_Z/\{[L_X^2\sin^2(\theta - \varphi) + L_Z^2\cos^2(\theta - \varphi)]KTc_g\},$$

or

$$n_p/n = (c/c_g)L_X L_Z/[L_X^2\sin^2(\theta - \varphi) + L_Z^2\cos^2(\theta - \varphi)],$$

since the phase speed, $c = 2\pi/KT$. The ratio can be written

$$n_p/n = (c/c_g)(W^2/L_X L_Z).$$

The number of waves observed as the group passes a fixed point, n_p, is therefore related to the number of waves within a group, n, multiplied by a term that depends both on c/c_g, as for surface waves, and also on a term that is a function of the group's shape.

Similar reasoning can be applied to find the number of waves recorded as an internal wave group passes a fixed vertical mooring line. The width of the elliptical group in the horizontal direction is $W = [L_X^2\cos^2\varphi + L_Z^2\sin^2\varphi]^{1/2}$, and the speed of the group in this direction is $c_g\cos\theta$. The time to cross the vertical mooring line is therefore $t = W/c_g\cos\theta$. The speed of the waves in the group in the horizontal direction normal to the mooring line is $c\sin\theta$ and their length in this direction is $2\pi/K\sin\theta$, where K is the wavenumber of the waves. The number of waves, n_m, crossing the mooring line as the group passes it in time t is therefore $ct\sin\theta/(2\pi/K\sin\theta)$, or $n_m = (c/c_g)(\sin^2\theta/\cos\theta)(WK/2\pi)$. Using (15) we can write

$$n_m/n = (c/c_g)(W/D)(\sin^2\theta/\cos\theta),$$

where $W/D = \{[L_X^2\cos^2\varphi + L_Z^2\sin^2\varphi]/[L_X^2\sin^2(\theta - \varphi) + L_Z^2\cos^2(\theta - \varphi)]\}^{1/2}$.

In general the ratio depends on the shape of the wave groups.

APPENDIX C

Generation of wave groups by a moving turbulent disturbance

Superimposed groups of waves are supposed to be generated as in Figure 1 by the motion of a disturbance of length L containing a variety of wavenumbers (i.e., a narrowband disturbance representing frozen turbulence) moving at a speed U for a time T_*, and that the disturbance components centered at wavelength λ generates a radiating internal wave group, one of which is shown in Figure A1 and described in the figure caption. Neglecting dispersion of the wave pattern over the time T_*, the group boundaries are, as shown, inclined to the horizontal at angle $-\Phi$, being generated as in Fig. 2. The number of waves of length λ produced is

$$n = (L + UT*)/\lambda, \tag{A2}$$

and so, defining $\chi = kU/N$ as before,

$$n = (1 + s)\chi/2\pi p, \tag{A3}$$

since $\lambda = 2\pi/k = 2\pi pL/\chi$, where $s = UT_*/L$, the distance traveled by the disturbance divided by its length L, and $p = U/NL$, say. The number of disturbance wavelengths in the moving packet of disturbances is $L/\lambda = \chi/2\pi p$, which must exceed unity. If $F = 0$, $\theta = \tan^{-1}[(\chi/(1 - \chi^2)^{1/2}]$ from (5) and $\Phi = -\tan^{-1}[(1 - \chi^2)^{1/2}/\chi]$ from (9), and so $\Phi = \theta - \pi/2$, and angle DAO $= \pi/2$. Now from the geometry of Fig. A1, if the angle DCA $= -\phi$ defines the group orientation, $\tan\phi = -\text{DA}\sin(-\Phi)/[\text{L} + \text{DA}\cos(-\Phi)]$. But DA $= UT_*\sin\theta$, and so

$$\phi = -\tan^{-1}[s\sin\theta\cos\theta/(1 + s\sin^2\theta)]. \tag{A4}$$

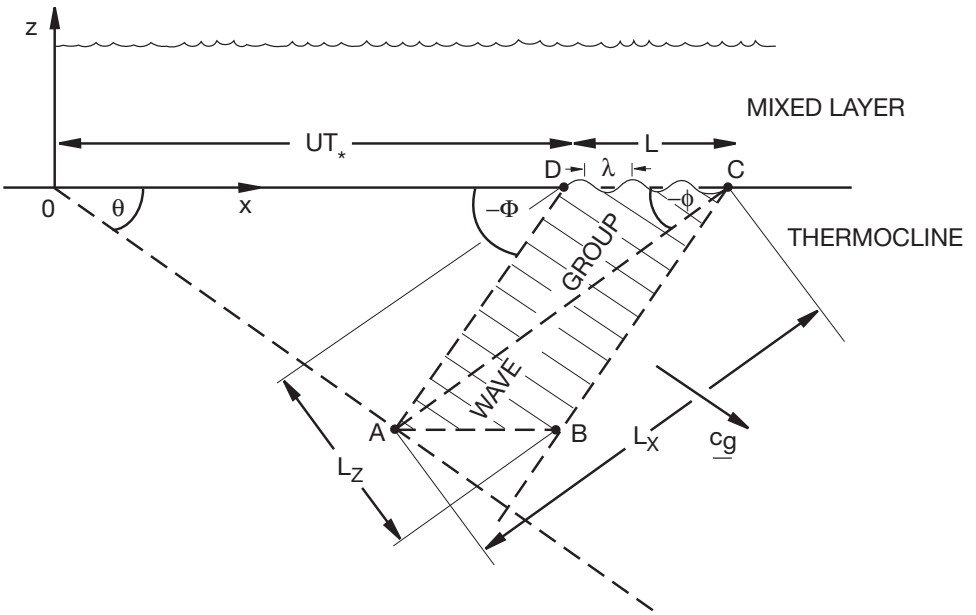

Figure A1. A group of waves generated by a disturbance of length L moving at speed U from O at x = 0 for a time T_*. The group is shown at the moment the disturbance ends. The bottom of the group defined by the line AB is formed when the disturbance, acting locally as a periodic plunger, moves at speed U from its initial location, $0 \le x \le L$ to $UT_*L \times UT_* + L$. The length of the wave crests (sketched as thin lines) is subsequently determined by the group velocity, c_g, and the duration of forcing at any location, i.e., by the time L/U in $0 \le x \le UT_*$. The length of the wave crests in $UT_* \le x \le UT_* + L$ (the latter beng point C) steadily reduces with x because the time over which the disturbance passes any point, x, (i.e., the time for which waves are generated) decreases to zero. The group is inclined to the horizontal at angle $-\phi$, with the longer, X, axis given by the line CA. At subsequent times, the group propagates in direction $\underline{c_g}$, moving downwards below the line z = 0 and separating from the x-axis.

Furthermore, $L_X = AC = UT_*\sin\theta\cos\theta/\sin(-\phi)$ and $L_Z = 2L\sin(-\phi)$, and so

$$q = L_Z/L_X = 2\sin^2\phi/(s\sin\theta\cos\theta), \tag{A5}$$

while

$$\delta_Z = L_Z/\lambda = -2n\sin\phi/(1+s). \tag{A6}$$

The vertical distance to which the centre of the wave groups reaches before dispersing, is made of two parts, the initial depth, $Z_1 = L_X \sin(-\varphi)/2 = (sL\sin\theta\cos\theta)/2 = (s\lambda\chi\sin\theta\cos\theta)/4\pi p$ as for the group shown in Figure A1, and that corresponding to its subsequent vertical motion before its component waves disperse, z_{max}. The total vertical distance, Z_{max}, is therefore given in nondimensional form as

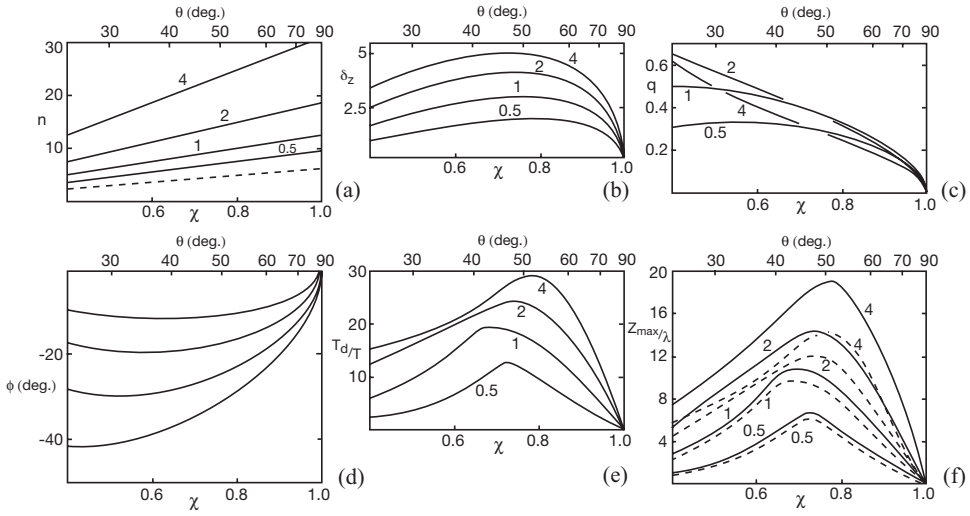

Figure A2. Vertical propagation of slanting groups generated by a disturbance in the mixed layer when $p = U/NL = 0.025$, $F = 0$ and at various values of $s = UT_*/L$ (labeled). (a) the number of waves in groups, n: the number of waves in the forcing disturbance are indicated by the dashed line; (b) the relative width, δ_Z; (c) the aspect ratio of groups, q; (d) the group orientation, ϕ; (e) the nondimensional duration of wave groups, T_d/T, expressed as a number of wave periods: and (f) the maximum depth of the centre of wave groups, Z_{max}/λ (full line) and the vertical motion, z_{max}/λ (dashed lines), all vs. χ and θ.

$$Z_{max}/\lambda = (s\chi\sin\theta\cos\theta)/4\pi p + z_{max}/\lambda, \tag{A7}$$

where z_{max}/λ is given by (18).

These parameter values are used to define wave groups generated by the moving disturbance over a range $0.4 \leq \chi \leq 1.0$ to cover the range in which the vertical component of group velocity is maximum. The parameter r is chosen to be 0.25, as before. Figure A2 shows values found by selecting $p = U/NL = 0.025$ with $s = UT_*/L = 0.5$, 1, 2 and 4, values indicated on the curves in the figure. Parts (a)–(d) show, respectively, the variations with χ (or θ) and with s of: the number of waves in a group, n (with the number of waves in the forcing disturbance being shown by the dashed line); the relative widths, δ_Z; the aspect ratio, q; and the orientation, ϕ. The number of waves increases linearly with χ as in (A3) and parameter δ_Z, given by (A6), increases with s. The aspect ratio, q, decreases as χ increase when $\chi > 0.55$. Groups have negative orientation (becoming more negative as s increases), just as do many of wave groups found to have the greatest duration in Section 3 (e.g., in Figs. 8 and 12), but neither δ_Z nor n remain constant as in Cases A or B. The duration of wave groups measured as the number of the periods of its component waves, T_d/T, found using (16), is shown in Fig. A2e. Maximum values lie between 12 and 30, increase with s, and are found between $\chi = 0.7$ ($\theta = 44.4$ deg.) and 0.78 ($\theta = 51.3$ deg.).

The depth to which groups travel are given in part (f), the full lines showing Z_{max}/λ and the dashed lines the vertical motion, z_{max}/λ. The total depth, Z_{max}, reaches largest values that increase with s and peak at values of χ in the same range as do T_d/T. Values of z_{max} peak at about the same values of χ as Z_{max}, and are generally the major contribution to Z_{max}. For some values of s (and p), however, substantial dispersion will occur to waves during the time T_* before the form of the group reaches the stage illustrated in Figure A2 and, because of dispersion during the time T_*, a factor ignored in this analysis, values of Z_1/λ—and consequently Z_{max}/λ—will be overestimated.

APPENDIX D

The orientation of scars produced by two-dimensional wave groups

Figure A3 shows an elliptical area, V, within which internal waves of a surrounding group are breaking. The area moves with the group velocity, $\underline{c_g}$, and the waves within the group break as they pass through V, their crests advancing at speed $\underline{c}$ (where underlined quantities denote vectors). As shown in Figure A3(a) the group velocity is inclined to the horizontal at an angle θ and the major axis of V is inclined to the horizontal at angle ϕ (assumed to be equal to that of the group containing the breaker region). A given point on a wave (e.g., the location of its maximum amplitude or where the shear it generates is greatest), moves with the wave at speed $\underline{c}$ but the wave is carried by the group at speed $\underline{c_g}$, and the point consequently moves through the fluid at speed $\underline{c_g} + \underline{c}$ (see Eq. 6) at an angle,

$$\alpha = \tan^{-1}\{F^2[(1 - \chi^2)/(\chi^2 - F^2)]^{1/2}\}, \tag{A8}$$

to the horizontal, where (5) is used to express θ in terms of χ. Because usually $F \ll 1$, this angle is generally very small except for near inertial waves when $\chi \approx F$ (or $\sigma/f \approx 1$). However, the central point of the length of a wave crest that is breaking (referred to, for simplicity, as the "breaking point"), which defines the center of a mixing region or "scar" left by the breakers, moves on a trajectory through the elliptical area, V, (i.e., relative to the ellipse, which itself moves with speed $\underline{c_g}$) between the points at which the waves enter and leave V. This trajectory is a straight line joining the points at which lines of slope θ (dotted in the figure and defining the orientation of lines of constant phase) touch the ellipse, V. The inclination, γ, of this line to the major axis of V is given by

$$\tan\gamma = q^2\cot(\text{angle OHG}), \tag{A9}$$

where q is the ratio of the minor and major and minor axes of V, respectively, assumed to be the same ratio as has the wave group containing the volume V within which the waves are breaking. But from triangle OHG, angle OHG $= \theta - \phi$, so

$$\gamma = \tan^{-1}[(q^2\cot(\theta - \phi)]. \tag{A10}$$

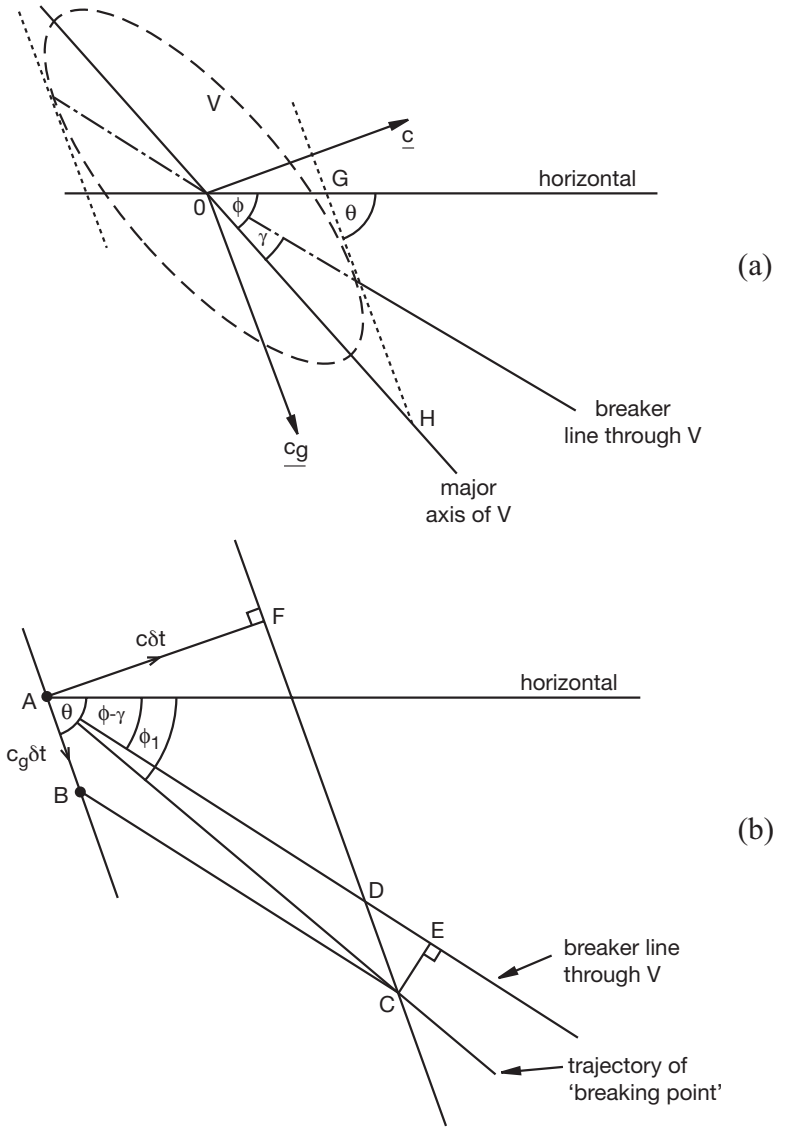

Figure A3. The trajectory of a breaking region. (a) The dashed elliptical line is the area, V, of a group within which waves break. Its major axis is inclined at angle ϕ to the horizontal, and it propagates with the group at the group velocity, $\underline{c_g}$. Individual waves, their constant phase lines parallel to $\underline{c_g}$, propagate in the direction and the speed of $\underline{c}$. The dash-dotted line marks the trajectory of the breaker point through the volume, V. (b) The motion of the breaker point from A to C in a time δt. In this time the wave has moved from AB to FDC and V has advanced a distance AB (or DC) equal to $c_g\delta t$. The line AD is parallel to the breaker trajectory relative to V. E is the projection of C onto the line AD.

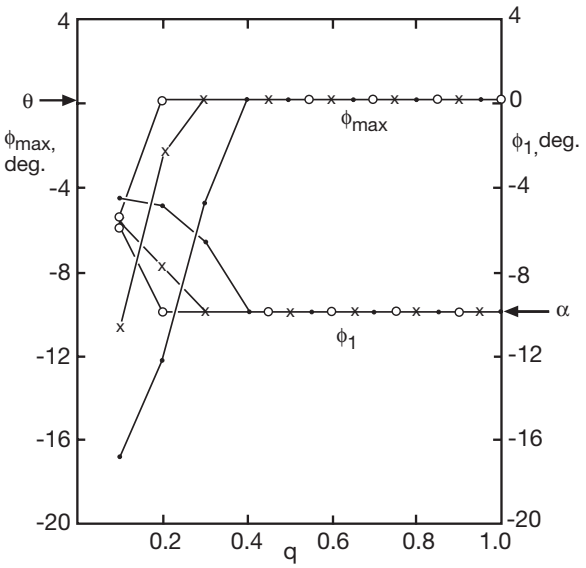

Figure A4. Near-inertial waves. The variation of the inclination to the horizontal of the scars, ϕ_1, and of the major axes of the groups, $\phi = \phi_{max}$, with the group shape parameter, $q = L_Z/L_X$, for two-dimensional ($r = 0$) groups in case A when their duration, T_d, is greatest, at values of $\delta_Z = L_Z/\lambda = 4$ (dotted points), 2 (crosses) and 1 (circles), as in Fig. 8, when $F = 10^{-2}$ and $\chi = 1.0017 \times 10^{-2}$. Values of the direction of the group velocity, θ, and the direction α of the vector $\underline{c} + \underline{c_g}$ (A8) are marked by arrows on the ϕ_{max} and ϕ_1 axis, respectively.

Figure A3b shows how a breaking point moves from A to C in a time δt as a line of constant phase in a wave, initially denoted by the line AB aligned in the direction $\underline{c_g}$, moves a distance $c\delta t$ to its new location, FDC, where AF = $c\delta t$. The line AD is the trajectory of A through V, and is inclined at angle $\phi - \gamma$ to the horizontal, as in part (a). The area V is however moving at speed $\underline{c_g}$, so that, in a time δt, the line AD within V moves to BC, where AB = DC = $c_g\delta t$, and C is the new location of the breaking point. The trajectory, AC, of the breaking point inclined at some angle, ϕ_1, to the horizontal, defines the orientation of scars left by breaking waves as they pass through the breaker area, V.

By simple geometry, angle BAD = $\theta - \phi + \gamma$ = angle ADF, and so, since angle AFD = $\pi/2$, AD = AF/sin(angle ADF) = $c\delta t/\sin(\theta - \phi + \gamma)$. Also if E is the projection of C onto AD, angle CDE = angle BAD, and so CE = CD sin(angle CDE) = $c_g\delta t \sin(\theta - \phi + \gamma)$ and DE = CD cos(angle CDE) = $c_g\delta t \cos(\theta - \phi + \gamma)$. It follows that since angle CAE = $\phi_1 - \phi + \gamma$, and tan(angle CAE) = CE/AE = CE/(AD+DE),

$$\phi_1 = \tan^{-1}\{2c_g\sin^2(\theta - \phi + \gamma)/[2c + c_g\sin(2(\theta - \phi + \gamma))]\} + \phi - \gamma. \qquad \text{(A11)}$$

Now using (4), (1) and (5), $c_g/c = \tan\theta\,(1 - F^2)/[\tan^2\theta + F^2]$ for two-dimensional groups when $l = 0$, and the scar inclination is therefore

$$\phi_1 = \tan^{-1}\{2\tan\theta(1-F^2)\sin^2(\theta-\phi+\gamma)/[2(\tan^2\theta+F^2) + \tan\theta(1-F^2)\sin(2(\theta-\phi+\gamma))]\} + \phi - \gamma, \quad \text{(A12)}$$

where γ is given by (A9).

When the major axis of V, and the group, is inclined at angle θ to the horizontal, $\phi = \theta$, so (A10) gives $\gamma = \pi/2$ (for all q), giving

$$\phi_1 = \tan^{-1}\{2\tan\theta(1-F^2)/[2(\tan^2\theta+F^2)]\} + \theta - \pi/2, \quad \text{(A13)}$$

and if $F = 0$, $\phi_1 = 0$; the scars are horizontal. Again, if alternatively $\phi = \theta + \pi/2$, as in the group sketched in Figure 2, it follows that $\phi_1 = 0$.

The scar angles, ϕ_1, are all found to be less than 2 deg for the two-dimensional groups of maximum duration, T_d, and inclination, ϕ_{max}, when $\chi = 0.1$, 0.2 and 0.4 as found in Fig. 8. For near-inertial waves, however, with $\phi_{max} \neq \theta$ much larger scar angles are found. Fig. A4 shows ϕ_{max} and ϕ_1 for $\chi = 1.0017 \times 10^{-2}$ when $F = 10^{-2}$, corresponding to $\theta = 0.0334$ deg and $\sigma/f = 1.0017$.

REFERENCES

Alford, M. and R. Pinkel. 2000. Observations of overturning in the thermocline: The context of ocean mixing. J. Phys. Oceanogr., *30,* 805–832.

Ansong, J. K. and B. R. Sutherland. 2010. Internal gravity waves generated by convective plumes. J. Fluid Mech., *648,* 405–434.

Borisenko, Yu. D., A. G. Voronovich, A. I. Leonov and Yu. Z. Miropolskiy. 1976. Towards a theory of non-stationary weakly nonlinear internal waves in a stratified fluid. Izv. Acad. Nauk USSR, English edn. Atmos. Ocean. Phy., *12,* 174–179.

Dohan, K. and B. R. Sutherland. 2003. Internal waves generated from a turbulent mixed region. Phys. Fluids, *15,* 488–498.

—— 2005. Numerical and laboratory generation of internal waves from turbulence. Dyn. Atmos. Oceans, *40,* 43–56.

Farmer, D. M. and M. Li. 1995. Patterns of bubble clouds organised by Langmuir circulation. J. Phys. Oceanogr., *25,* 1425–1440.

Gayen, B., S. Sarkar and J. R. Taylor. 2010. Large eddy simulation of a stratified boundary layer under an oscillatory current. J. Fluid Mech., *643,* 233–266.

Hunt, J. N. 1961. Interfacial waves of finite amplitude. La Houille Blanche, *16,* 515–531.

Lighthill, J. 1978. "Waves in Fluids." Cambridge University Press, Cambridge. 504 pp.

Linden, P. F. 1975. The deepening of a mixed layer in a stratified fluid. J. Fluid Mech., *71,* 385–405.

Lombard, P. N. and J. J. Riley. 1996. On the breakdown into turbulence of propagating internal waves. Dyn. Atmos. Oceans, *23,* 345–355.

Mathur, M. and T. Peacock. 2009. Internal wave beam propagation in non-uniform stratifications. J. Fluid Mech., *639,* 133–152.

McWilliams, J. C., P. P. Sullivan and C.-H. Moeng. 1997. Langmuir turbulence in the ocean. J. Fluid Mech. *334,* 31–58.

Mowbray, D. E. and B. S. H. Rarity. 1967. A theoretical and experimental investigation of the phase configuration of internal waves of small amplitude in a density stratified liquid. J. Fluid Mech., *28,* 1–16.

Pham, H. T., S. Sarkar and K. A. Brucker. 2009. Dynamics of a stratified shear layer above a region of uniform stratification. J. Fluid Mech., *630,* 191–223.

Polton, J. A., J. A. Smith, J. A. MacKinnon and A. E. Tejada-Martinez. 2008. Rapid generation of high-frequency internal waves beneath a wind and wave forced oceanic surface mixed layer. Geophys. Res. Lett., *35,* L13602, doi:10.1029/2008GL033856.

Smith, J. A. and C. Brulefert. 2010. Persistent wave groups. J. Phys. Oceanogr., *40,* 67–84.

Smith, J., R. Pinkel and R. A. Weller. 1987. Velocity structure in the mixed layer during MILDEX. J. Phys. Oceanogr., *17,* 425–439.

Staquet, C. and F. S. Godeferd. 1998. Statistical modelling and direct numerical simulation of decaying stably stratified turbulence. Part I. Flow energetics. J. Fluid Mech., *360,* 295–340.

Staquet, C. and J. Sommeria. 2002. Internal gravity waves: from instabilities to turbulence. Annu. Rev. Fluid Mech., *34,* 559–593.

Sutherland, B. R. 2001. Finite-amplitude internal wavepacket dispersion and breaking. J. Fluid Mech., *429,* 343–380.

—— 2006. Weakly nonlinear internal gravity wavepackets. J. Fluid Mech., *569,* 249–258.

Sutherland, B. R. and P. F. Linden. 1998. Internal wave excitation from a stratified flow over a thin barrier. J. Fluid Mech., *377,* 223–252.

Taylor, J. R. and S. Sarkar. 2007. Internal gravity waves generated by a turbulent bottom Ekman layer. J. Fluid Mech., *590,* 331–354.

Thorpe, S. A. 1975. The excitation, dissipation, and interaction of internal waves in the deep ocean. J. Geophys. Res., *80,* 328–338.

—— 1977. On the stability of internal wavetrains, *in* A Voyage of Discovery: George Deacon 70th Anniversary Volume, M. Angel, ed., Pergamon Press, Oxford, 199–212.

—— 1992. The break-up of Langmuir circulation and the instability of an array of vortices. J. Phys. Oceanogr., *22,* 350–360.

—— 1994. Statically unstable layers produced by overturning internal gravity waves. J. Fluid Mech., *260,* 333–350.

—— 1999. On internal wave groups. J. Phys. Oceanogr., *29,* 1085–1095.

—— 2002a. On the dispersion of pairs of internal inertial gravity waves. J. Mar. Res., *60,* 461–476.

—— 2002b. The axial coherence of Kelvin-Helmholtz billows. Quart. J. Roy. Meteorol. Soc., *128,* 1529–1542.

—— 2005. The Turbulent Ocean, Cambridge University Press, Cambridge, 439 pp.

Thorpe, S. A. and A. J. Hall. 1982. Observations of the thermal structure of Langmuir circulation. J. Fluid Mech., *114,* 237–250.

Troy, C. D. and J. R. Koseff. 2005. The instability and breaking of long internal waves. J. Fluid Mech., *543,* 107–136.

Received: *5 April, 2010;* revised: *17 August, 2010.*